Petroleum Science 21 (2024) 3029–3046

Contents lists available at ScienceDirect

Petroleum Science

journal homepage: www.keaipublishing.com/en/journals/petroleum-science

Original Paper

Biological origin and depositional environment of crude oils in the Qiongdongnan Basin: Insights from molecular biomarkers and whole oil carbon isotope

Zi-Ming Zhang [a, b, c], Du-Jie Hou [a, b, c, *], Xiong Cheng [a, b, c], Da-Ye Chen [d], Gang Liang [e], Xia-Ze Yan [a, b, c], Wei-He Chen [a, b, c]

[a] School of Energy Resources, China University of Geosciences, Beijing, 100083, China
[b] Key Laboratory of Marine Reservoir Evolution and Hydrocarbon Accumulation Mechanism, Ministry of Education, Beijing, 100083, China
[c] Beijing Key Laboratory of Unconventional Natural Gas Geological Evaluation and Development Engineering, Beijing, 100083, China
[d] China Coal Research Institute, Beijing, 100013, China
[e] Exploration and Development Resource Institute, Hainan Branch of China National Offshore Oil Corporation, Haikou, 570300, Hainan, China

ARTICLE INFO

Article history:
Received 15 December 2023
Received in revised form
4 April 2024
Accepted 30 May 2024
Available online 3 June 2024

Edited by Jie Hao and Meng-Jiao Zhou

Keywords:
Gas chromatography-mass spectrometry
Molecular biomarker
Simonellite
Biological source
Depositional environment

ABSTRACT

Molecular biomarker and whole oil carbon isotope ($\delta^{13}C_{oil}$) analyses were conducted on eleven typical crude oils from the Qiongdongnan Basin to investigate their biological sources and depositional environments. Saturated hydrocarbon biomarkers in most samples are characterized by angiosperm-derived compounds, with aromatic compounds dominated by the naphthalene, phenanthrene, biphenyl, and fluorene series. The related source rocks of these oils were mainly deposited under oxic condition, but a subanoxic–suboxic and enclosed water column condition in the Central Depression during Oligocene. The identification of simonellite and related compounds in the aromatic fractions provides reliable evidence for the input of coniferous gymnosperms. Cadalene may also have a potential association with gymnosperms since it shows a strong positive correlation with simonellite. Evidence from density, n-alkanes, short-chain alkylbenzenes and secondary brine inclusions indicates that the unique crude oil B13-1 may have suffered from thermal alteration. These crude oils (excluding B13-1) can be classified into four types based on the $\delta^{13}C_{oil}$ values and molecular biomarkers. Type A oil (solely S34-3) is characterized by non-angiosperm plants, with minor dinoflagellates and increasing contribution from conifer gymnosperms than others. Type B oils (L17-2, L18-1, L25-1, and L25-1W) show heavy $\delta^{13}C_{oil}$ (−24 ‰ to −25 ‰) and mixed contributions from both angiosperms and marine algae, with the marine algae contribution increasing. Type C oils (L13-2 and B21-1) share similar biological sources with Type B, but the moderately δ^{13}Coil (−25‰ to −26‰) and high level of terrestrial biomarkers suggesting a predominant contribution of angiosperms. Type D oils (Y13-1a, Y13-1b, and Y13-4) possess the lightest $\delta^{13}C_{oil}$ (mainly below −26‰) and are primarily derived from angiosperms, with mangrove vegetation playing an important role. Spearman correlation analysis among 14 source biomarker parameters with $\delta^{13}C_{oil}$ and geological setting of related source rocks implied that the marine algae should be responsible for the heavy $\delta^{13}C_{oil}$ in the Type B. The contribution of marine algae in the Central Depression may have been neglected in the past, as it is usually covered by remarkable angiosperm biomarkers.

1. Introduction

The Qiongdongnan Basin is one of the important petroliferous basins in the northern part of South China Sea, it was believed that terrestrial organic material from angiosperms dominated the source rock during the early exploration of shallow-water area (Huang et al., 2003; Zhou et al., 2003; Xiao et al., 2006). With a series of breakthroughs in the deep-water area, more attention has gradually turned to the widespread Oligocene marine terrigenous source rock (Li and Zhang, 2017; Wu et al., 2018). A great deal of

* Corresponding author.
E-mail address: houdj313@163.com (D.-J. Hou).

https://doi.org/10.1016/j.petsci.2024.05.026

analyses on natural gases and saturated hydrocarbon biomarkers of oils have been conducted to investigate the geochemical characteristics of marine terrigenous source rocks in the Central Depression, but less attention has been devoted to the composition of aromatic compounds (Zhu et al., 2018). Angiosperms transported by fluvial-delta systems were considered the primary source of crude oils in deep-water areas, supported by the high abundances of oleanane and bicadinanes in the Central Depression (Huang et al., 2017). However, credible evidences for the apparent contradiction between the biased $\delta^{13}C_{oil}$ and the significant angiosperm indicators in the Central Depression are currently absent. Aromatic biomarkers record substantial geological information with less susceptibility to maturation, and they have been widely employed in petroleum geology to investigate the depositional environment and organic matter source (Püttmann and Villar, 1987). For example, the 1,2,7-trimethylnaphthalene is considered to be derived from angiosperms, simonellite is exclusively indicative of coniferous gymnosperms (Simoneit et al., 1986; Strachan et al., 1988), and heterocyclic compounds are valuable in depositional environmental discrimination (Hughes et al., 1995; Radke et al., 2000; Liu et al., 2022).

In this study, we conducted systematic analyses of molecular biomarkers on eleven representative crude oils from the Qiongdongnan Basin. We clarified the correlation between carbon isotopes and biological source material, discussed the source composition of different types of crude oils, and inferred the Depositional environment of the marine terrigenous source rock in the Central Depression.

2. Geological background

The Qiongdongnan Basin is located in the northern continental margin of the South China Sea, it is an extensional sedimentary basin developed on the background of a Cenozoic fault depression and quasi-passive continental margin, with an area of approximately 80,000 km^2 (Hutchison, 2004; Hayes and Nissen, 2005). The water depth line divided this basin into deep and shallow-water area, with the deep-water area covering about 53,000 km^2 (Zhou et al., 2008; Zhu et al., 2009). The tectonic framework of the basin is divided into three depressions by fault No. 2 and No. 11 (Fig. 1). The Northern Depression contains Yabei, Songxi and Songdong Sags. The Central Depression contains Ledong, Lingshui, Beijiao, Songnan, Baodao and Changchang Sags. The Southern Depression contains Huaguang and Ganquan Sags. The pre-Paleogene igneous rocks, metamorphic rocks and sedimentary rocks constitute the basement of this basin (Huang et al., 2003; Lai et al., 2021). The Qiongdongnan Basin has experienced the rifting stage (T100–T70), rifting-downwarping stage (T70–T60), thermal subsidence stage (T60–T30) and rapid subsidence stage (T30–) with a typical double-layer structure (Zhou et al., 2008; Lei et al., 2011).

Due to the rapid deposition rate, the Qiongdongnan Basin has developed an extensive Cenozoic stratum, reaching a thickness of up to 12,000 m. The stratum distributions from old to new are Lingtou formation, Yacheng formation, Lingshui formation, Sanya formation, Meishan formation, Huangliu foumation, Yinggehai formation and Ledong formation (Lai et al., 2021; Zhu et al., 2021). It is believed that hydrocarbons in the Qiongdongdong Basin are mainly generated by three types of source rocks: the Eocene lacustrine source rock, the Oligocene marine-continental transitional coal measure source rock, and the Oligocene shallow marine mudstones. Among these, the distribution of Eocene lacustrine source rock is mainly limited in the Northern Depression. The Oligocene shallow marine mudstones are also known as marine terrigenous source rock due to the input of terrigenous organic matter (Wang et al., 2014, 2020; Zhu et al., 2021). Although the TOC of the marine terrestrial source rocks is relatively low, it still has great hydrocarbon potential because of the substantial thickness and widespread distribution in the Central Depression (Wu et al., 2018). The Oligocene marine-continental transitional coal measure source rocks are believed to be the main source of YC13 gas field in the shallow water (Huang et al., 2003; Xiao et al., 2006). The organic matter type of source rock in the Qiongdongnan Basin is classified as II_2–III, predominantly associated with gas generation and supplemented by oil generation (Huang et al., 2016). After half a century of exploration and development, a series of giant gas fields and hydrocarbon-bearing structures have been established, such as YC13-1, YC13-4, LS13-2, LS17-2, LS18-1, LS18-2, LS22-1, LS25-1, LS25-1W, YL8-3, BD21-1 gas fields, the proved geological reserves of natural gas are more than 300 billion m^3 (Xu et al., 2023a).

3. Materials and methods

3.1. Sample introduction

A detailed organic geochemical investigation of eleven crude oils was undertaken, which distributed in Songdong, Ya'nan, Baodao, Lingshui and Ledong Sags of the Qiongdongnan Basin. The specific locations of them are shown in Fig. 1(a), while the geological background and bulk characteristics are presented in Table 1. The density of samples ranges from 0.7151 to 0.8502 g/cm^3, which mainly belongs to condensate or light oil. Most samples are low-wax oils except sample Y13-1a. All samples are low-sulfur crude oils. The bulk compositional of saturated fractions, aromatic hydrocarbons (Aro), polar compounds and asphaltenes (NOS + Asp) concentrations fall within the range of 75.2%–96.7%, 1.2%–15.7%, 2.1%–10%, respectively.

3.2. Methods

The separation of saturated and aromatic fractions was performed using alumina liquid chromatography columns. A glass column was packed with activated (8 h, 450 °C) alumina powder (100–150 mesh, approx. 25 g). The removal of precipitated asphaltene was done to minimize the loss of lightweight components. A large amount of 200–250 mg crude oil samples were fractionated into saturated fractions by elution with n-Hexane (approx. 60 mL) initially, followed by the elution of aromatic hydrocarbons using a mixed solvent of dichloromethane and n-Hexane (2:1, v/v, approx. 40 mL) according to the industry standard SY/T 5119-2016. The aromatic fractions were concentrated to 5 mL in preparation for GC-MS analysis.

GC analysis of pristane and phytane in the saturated fractions were performed using an Agilent 7890A gas chromatograph equipped with an HP-5 column. Nitrogen served as the carrier gas. The oven temperature started at 40 °C for an initial isothermal period of 2 min, then increased to 300 °C at a rate of 4 °C/min and held for 20 min.

GC-MS analysis of saturated and aromatic fractions was performed on an Agilent 7890A GC coupled to a 5975C mass spectrometer and equipped with an HP-5MS (60 m × 0.25 mm × 0.25 μm) fused silica capillary column. Helium was used as the carrier gas with a constant flow rate of 1.5 mL/min. The GC operating conditions were as follows: the inlet temperature was set to 300 °C, the oven was heated from 40 °C to 300 °C at a programed rate 3 °C/min and then holding for 30 min. The electron ionization energy of MS ion source was 70 eV, the data acquisition mode was full scan with a mass range from *m/z* 50 to 600. Biomarker identification was based on comparison of mass spectra

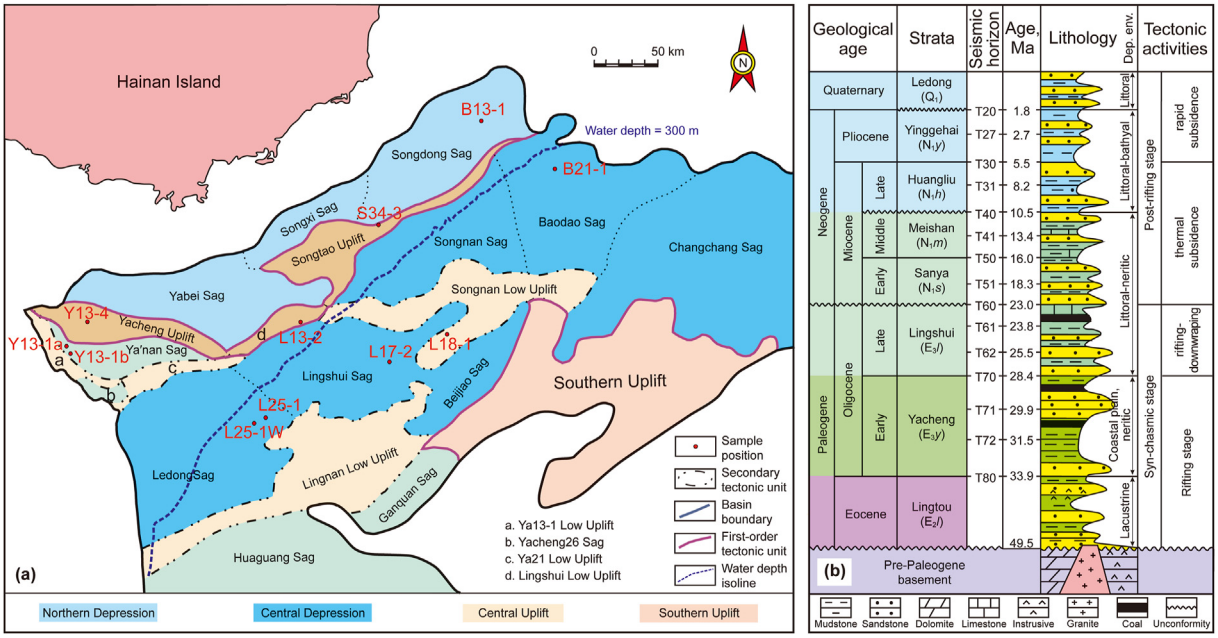

Fig. 1. **(a)** Geological profile map of the Qiongdongnan Basin and the locations of crude oils mentioned in this study. **(b)** Generalized stratigraphic column of the Qiongdongnan Basin. Dep. env. represents the depositional environment.

Table 1
Geological information and bulk characteristics of crude oils in the Qiongdongnan Basin.

Name	Location	Formation	Depth, m	Density, g/cm^3	Wax, %	Sulfur, %	Sat, %	Aro, %	NOS + Asp, %
S34-3	Songdong Sag	N_1s	2566–2644	0.7930	0.238	0.0258	91.8	3.4	4.8
L17-2	Lingshui Sag	N_1h	3777–3786	0.8183	0.125	0.0387	84.0	6.0	10.0
L18-1	Lingshui Sag	N_2y	2820–2847	0.7763	0.306	0.0307	89.9	4.2	5.9
L25-1	Lingshui Sag	N_1h	3961	0.8159	1.540	0.0443	94.4	2.8	2.9
L25-1W	Lingshui Sag	N_1h	3761–3767	0.8027	0.396	0.0296	91.3	3.4	5.3
B13-1	Songdong Sag	N_1m_2	1573–1580	0.7151	0.024	0.0200	96.7	1.2	2.1
B21-1	Baodao Sag	E_3l_3	4092–4155	0.8183	1.410	0.0334	75.2	15.7	9.1
L13-2	Lingshui Sag	N_1m_2	3778–3786	0.7828	0.646	0.0319	81.3	11.1	7.5
Y13-1a	Ya'nan Sag	E_3l_2	3898–3922	0.8502	9.030	0.0420	88.3	3.8	7.8
Y13-1b	Ya'nan Sag	E_3l_3	3775–3818	0.7928	1.030	–	91.4	3.4	5.2
Y13-4	Ya'nan Sag	N_1s_1	–	0.8096	0.730	–	85.2	6.0	8.8

Sat, Aro and NOS + Asp represent the saturated fractions, aromatic fractions, and polar compounds plus asphaltenes, respectively. These are determined based on the thin-layer chromatography.

with standard spectra in the NIST library and spectra interpretation.

GC-MS/MS analyses were performed on a Trace GC Ultra–TSQ Quantum XLS with a DB-5MS column (30 m × 0.25 mm × 0.25 μm). The mass spectrometer operated in parent ion mode, with argon used as the collision gas at a collision pressure of ca. 0.5 Torr, and a collision energy of 10 eV. The GC temperature program was as follows: hold for 1 min at 50 °C, ramp to 100 °C at 20 °C/min, then ramp to 315 °C at 3 °C/min and hold for 16 min at 315 °C.

The whole oil stable carbon isotope analyses were carried out on a Thermo Fisher MAT253 coupled to a Flash EA 1112. The reaction furnace temperature was set to 980 °C, and the ion source voltage was maintained at 3.07 kV. Each sample was analyzed at least twice to ensure an error of less than 0.1‰.

4. Results

4.1. Carbon isotope characteristics

The distribution of the $\delta^{13}C_{oil}$ ranged from −26.8‰ to −24.1‰ in the Qiongdongnan basin. Three oils (Y13-1a, Y13-1b, and Y13-4) from the Yacheng area exhibited the relatively light $\delta^{13}C_{oil}$ mainly lower than −26‰. The oils from the western part of Central Depression (L17-2, L18-1, L25-1, and L25-1W) and Songdong Sag (S34-3), possessed relatively heavy $\delta^{13}C_{oil}$ ranging from −25‰ to −24‰. Sample B13-1, B21-1, and L13-2 showed moderately $\delta^{13}C_{oil}$ ranging from −26‰ to −25‰. The distribution pattern of n-alkane carbon isotopes in all crude oils was similar (Zhu et al., 2018), becoming heavier with decreasing carbon numbers.

4.2. Saturated biomarkers

The distributions of saturated hydrocarbon biomarkers were presented in Fig. 2 and the corresponding parameters were listed in Table 2. The carbon number of n-alkanes in crude oils from the Qiongdongnan basin ranged from n-C_9 to n-C_{31}. These n-alkanes showed a smooth distribution without odd-even preference. Most samples were dominated by low to moderate carbon-number n-alkanes and no obvious main peaks. Pristane is prevalent in all samples, with Pr/Ph ratios ranging from 3.7 to 7.62. The $C_{19}TT/C_{30}H$

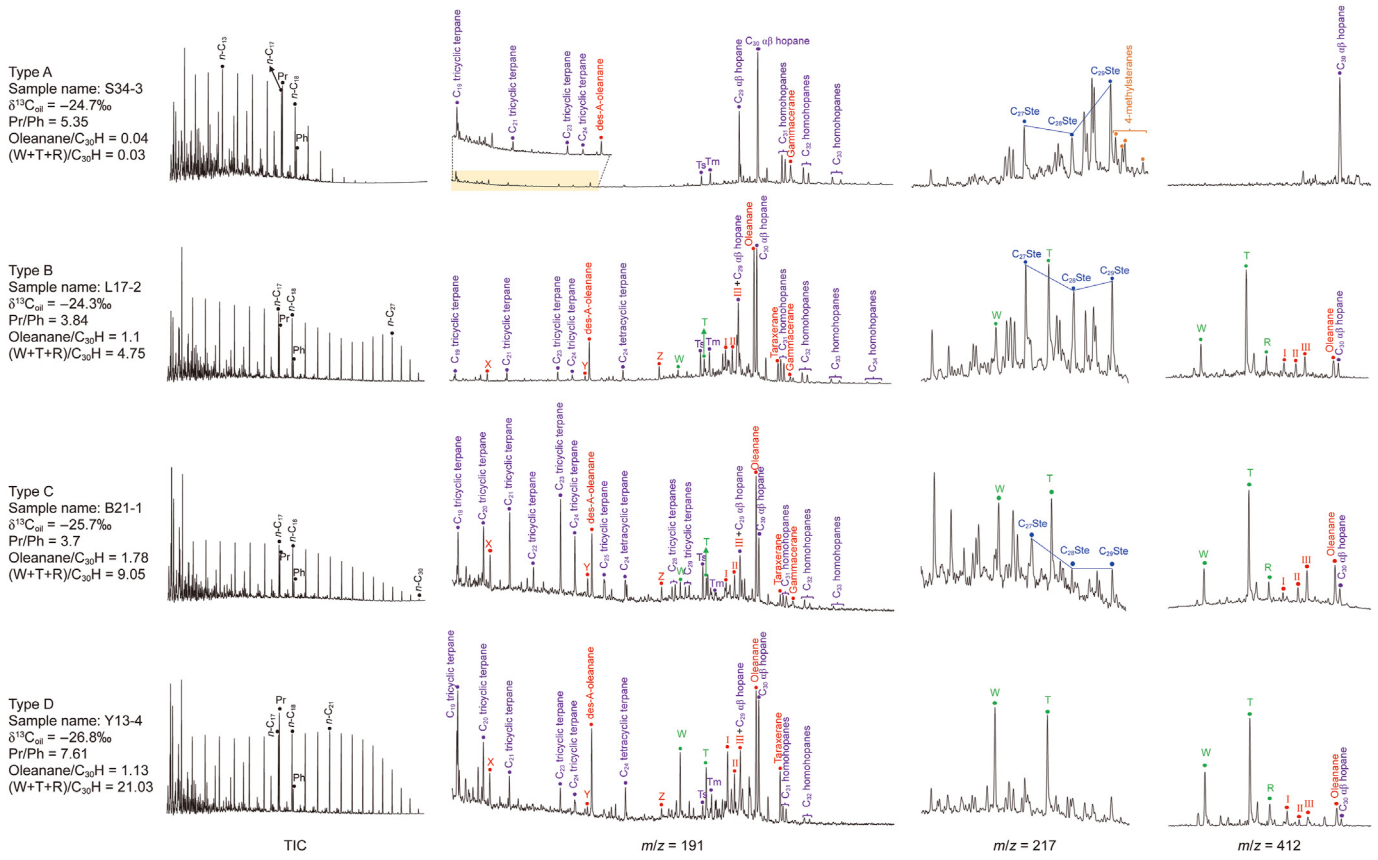

Fig. 2. Partial mass chromatograms of saturated hydrocarbon biomarkers for typical samples. Compounds I, II, and III are identified into rearranged oleananes (Nytoft et al., 2010). Compounds X, Y, and Z are triterpanes derived from oleananes (Samuel et al., 2010). W, T, T1 and R are bicadinanes.

Table 2
$\delta^{13}C_{oil}$ and saturated hydrocarbon biomarker parameters of crude oils in the Qiongdongnan basin.

Name	S34-3	L17-2	L18-1	L25-1	L25-1W	B13-1	B21-1	L13-2	Y13-1a	Y13-1b	Y13-4
$\delta^{13}C_{oil}$, ‰	−24.7	−24.3	−24.4	−24.1	−24.6	−25.8	−25.7	−25.3	−25.8	−26.1	−26.8
Pr/Ph[a]	5.35	3.84	4.01	4.08	4.17	6.50	3.70	5.38	7.62	5.63	7.61
Pr/n-C_{17}[a]	1.09	0.68	0.76	0.73	0.89	1.77	0.78	0.90	1.77	1.25	1.55
Ph/n-C_{18}[a]	0.31	0.21	0.23	0.22	0.27	0.41	0.26	0.21	0.26	0.25	0.22
$C_{19}TT/C_{30}H$	0.06	0.05	0.46	0.08	0.25	0.08	0.65	0.09	1.51	1.08	0.65
$C_{23}TT/C_{30}H$	0.02	0.06	0.62	0.09	0.17	0.13	1.17	0.09	0.41	0.37	0.16
Oleanane/$C_{30}H$	0.04	1.10	1.20	1.21	1.38	0.24	1.78	1.35	2.19	1.66	1.13
Taraxerane/$C_{30}H$	–	0.17	0.10	0.13	0.12	0.05	0.18	0.30	0.35	0.50	0.45
Gammacerane/$C_{30}H$	0.23	0.05	0.04	0.07	0.06	0.09	0.19	0.05	–	–	–
(W + T + R)/$C_{30}H$	0.03	4.75	11.99	4.84	5.53	0.36	9.05	9.51	76.59	98.50	21.03
C_{32}–C_{35} homohopanes/$C_{30}H$	0.43	0.31	0.07	0.33	0.23	0.24	0.41	0.14	0.13	0.19	0.08
2α-methylhopane/$C_{30}H$	–	0.45	0.86	0.61	0.42	0.07	0.90	0.99	–	–	–
C_{27} regular steranes%[b]	26.8	39.0	49.1	37.9	40.1	38.1	49.6	38.4	33.8	39.1	47.1
C_{28} regular steranes%[b]	22.7	31.2	35.0	30.9	31.3	37.5	21.9	26.7	15.0	20.9	29.0
C_{29} regular steranes%[b]	50.5	29.8	15.9	31.2	28.6	24.4	28.5	34.9	51.2	40.0	23.9
C_{29} S/(S + R)[b]	0.40	0.36	0.28	0.40	0.34	0.25	0.48	0.49	0.50	0.50	0.37
Type	A	B	B	B	B	–	C	C	D	D	D

$C_{30}H$ represents C_{30} αβ hopane; $C_{19}TT$ and $C_{23}TT$ represent C_{19} tricyclicterpane and C_{23} tricyclicterpanep; W, T and R represent bicadinanes; $C_{19}TT/C_{30}H$, $C_{23}TT/C_{30}H$, Oleanane/$C_{30}H$, Taraxerane/$C_{30}H$, Gammacerane/$C_{30}H$, C_{32}–C_{35} homohopanes/$C_{30}H$, 2α-methylhopane/$C_{30}H$ ratios were calculated using peak areas in the *m/z* 191 mass chromatograph; (W + T + R)/$C_{30}H$ ratio was calculated using peak areas in the *m/z* 412 mass chromatograph; C_{27} regular steranes% = C_{27} regular steranes/C_{27}–C_{29} regular steranes; C_{28} regular steranes% = C_{28} regular steranes/C_{27}–C_{29} regular steranes; C_{29} regular steranes% = C_{29} regular steranes/C_{27}–C_{29} regular steranes; C_{29} S/(S + R) = C_{29} 5(α), 14(α), 17(α), 20S-/C_{29} 5(α), 14(α), 17(α), (20S + 20R)-sterane.

[a] Data from GC.

[b] Data from GC-MS/MS.

ratios of these crude oils varied from 0.05 to 1.51, and the $C_{23}TT/C_{30}H$ ratios ranged from 0.02 to 1.17. The distribution of tricyclicterpanes differed significantly among these crude oils, with $C_{23}TT$ being dominant in oils L17-2, L18-1, L25-1, L25-1W, B21-1, and L13-2, while $C_{19}TT$ prevails in oils Y13-1a, Y13-1b, Y13-4, and S34-3. Gammacerane was detected with relatively low abundances

in all crude oils except for oils Y13-1a, Y13-1b, and Y13-4. The Gammacerane/C_{30}H ratios ranged from 0.04 to 0.23, with a mean value of 0.1. The C_{34} and C_{35} homohopanes of most crude oils could not be identified on the *m/z* 191 mass chromatogram (Fig. 2), significant variations in homohopanes composition are still observed. The C_{32}–C_{35} homohopanes/C_{30}H ranged from 0.08 to 0.43, with a mean value of 0.23.

Regular steranes were analyzed by GC-MS/MS to eliminate interference from triterpenoids. The proportion of C_{27} regular steranes to the total steranes ranged from 26.8% to 49.6% with an average of 40%, while C_{29} regular steranes ranged from 15.9% to 50.5% with an average of 33%. Low abundance of 4-methylsteranes was solely identified in oil S34-3. The sterane isomerization parameter C_{29} S/(S + R) ranged from 0.25 to 0.50 with a mean value of 0.39, reflecting a low to mature stage of these crude oils. The maturity of oil B13-1 was determined to be the lowest based on sterane isomerization parameters, and will be discussed in the following text.

Oleanane, des-A-oleanane, XYZ compounds and rearranged oleanane (I, II, and III in Fig. 2) were widely detected in the Qiongdongnan Basin. The Oleanane/C_{30}H ratio was used to characterize their relative abundance in these crude oils, ranging from 0.04 to 2.19, with a mean value of 1.2. Only sample S34-3 exhibited an unusually low abundance of oleanane. Taraxerane was observed in all samples except for S34-3, and the Taraxerane/C_{30}H ratios ranged from 0.05 to 0.5 with a mean of 0.24, in which it was significantly higher in crude oils Y13-1a, Y13-1b, and Y13-4. Another important group of triterpenoid compound in the Qiongdongnan Basin were bicadinanes, including compounds W, T, and R, which were notably prominent in the *m/z* 191 and *m/z* 217 mass chromatograms of some samples. The (W + T + R)/C_{30}H ratio was commonly used to characterize the relative abundance of bicadinanes showing substantial variation from 0.03 to 98.5. Similar to oleanane, bicadinanes in sample S34-3 could hardly be recognized at *m/z* 412 mass chromatogram, while they are remarkably high in other oils.

Surprisingly, we identified a series of methylhopanes (Fig. 3) in certain crude oils distributed exclusively within the Central Depression. These methylhopanes are dominated by high abundance of C_{31} 2α-methylhopane with lower levels of C_{32}–C_{35} 2-methyhopanes and C_{31} 3β-methylhopane, similar to the composition of homohopanes. The 2α-methylhopane/C_{30}H ratios ranged from 0.07 to 0.99 with a mean value of 0.61.

4.3. Bulk compositions of aromatic hydrocarbon

Alkylbenzenes are the most volatile aromatic compounds in crude oil, and their loss during the fraction separation is inevitable. All crude oils in this paper were separated in a same batch. Aromatic fractions from three times control experiments conducted on sample B21-1 showed highly consistent total ion chromatograms (see supplementary data). More complete distribution of naphthalene series compared with previous research (Zhu et al., 2018) confirmed the reliability of our oil separation and GC-MS analyses.

The distributions of aromatic compounds were shown in Fig. 4 and the corresponding parameters were presented in Table 3. A series of mono- to tetra-aromatic compounds were identified in these crude oils, mainly including alkylbenzenes, the naphthalene series, the phenanthrene series, the biphenyl series, the anthracene series, cadalene, retene, simonellite, the fluoranthene series, the pyrene series, the chrysene series, the phenylnaphthalene series, triaromatic steroids, the fluorsene series, the dibenzothiophene series, the dibenzofuran series, the triphenyl series. Due to the inevitable loss during fraction separation, the geological significance of alkylbenzenes would not be discussed in this paper. It should be noted that the sample B13-1 exhibits an unusually high content of alkylbenzenes (81%). Furthermore, this sample also shows the highest MPI in contrast to the C_{29} sterane isomerization ratio (Table 2), reflecting a maturity conflict, the reasons will be discussed later.

Aromatic hydrocarbon compositions of these samples were characterized by wide variations, with the top five (excluding alkylbenzenes) being typically naphthalene, phenanthrene, biphenyl, fluoranthene, and dibenzothiophene series. The naphthalene series had the highest content in all samples, ranging from 54% to 71.8%, with a mean value of 61.1%. The phenanthrene series ranged from 1.2% to 16.1%, with an average of 9.7%. The biphenyl series show a range of 7.6%–13.8%, with a mean value of 10.8%. The fluoranthene series ranged from 1.05% to 5.64%, with a mean value of 3.6%. The dibenzothiophene series ranged from 1.52% to 3.71%, with a mean value of 2.85%. Oils S34-3, Y13-1a, Y13-1b, and Y13-4 contained significantly lower levels of the phenanthrene series compared with other samples.

4.4. Bi- and tri-aromatic hydrocarbons

The bi- and tri-aromatic hydrocarbons (PAHs) were the predominant compounds in these samples, mainly comprising naphthalene, phenanthrene, biphenyl, cadalene and their alkyl or phenyl derivatives (Fig. 5). The naphthalene series included naphthalene, methylnaphthalenes, dimethylnaphthalene, trimethylnaphthalene, tetramethylnaphthalene, and pentamethylnaphthalene, with the abundance of alkylnaphthalenes decreasing as the number of alkyl groups increased (Fig. 6(a) and (b)). All crude oils exhibited a similar distribution of MNs, with peak 2-MN slightly higher than 1-MN. The DMN of all samples are dominated by high abundance of 2,6- + 2,7-DMN, 1,3- + 1,7-DMN and 1,6-DMN. The distribution of TMNs was characterized by high contents of 1,3,6-TMN and 1,2,7- + 1,6,7-TMN. The 1,2,7-/1,3,7-TMN ratio ranged from 0.28 to 0.65, with a mean value of 0.4. The highest abundance of TeMNs pointed to 1,3,6,7-TeMN.

Cadalene was detected in all samples with highly variable abundances. Since it was usually detected at the *m/z* 198 mass chromatogram (Fig. 6(a)), Cad/MDBTs was used to characterize its relative abundance in this paper. The Cad/MDBTs ratios ranged from 0.03 to 26.69 with a mean value of 3.21. In particular, cadalene in samples S34-3 was unusually high, and even outstanding on the TIC (Fig. 6(a)).

The phenanthrene series include phenanthrene, methylphenanthrenes, dimethylphenanthrenes, trimethylphenanthrenes and anthracene (Fig. 6(b)). The internal compositional features of phenanthrene series were less variable, with phenanthrene being the highest individual compound. The distribution of the MPs contents was disordered, with higher abundances of 9-MP, 3-MP and 2-MP and the lowest relative abundance of 1-MP. The DMPs characteristic in all the samples was relatively similar, with the 1,3- + 3,9- + 2,10- + 3-10-DMP peak was the highest on the *m/z* 206 mass chromatogram. The contents of TMPs and anthracene were very low.

It was notably that simonellite, retene, 6-isopro-pyl-1-isohexyl-2-methylnaphthalene and 1,2,3,4-tetrahydroretene were detected in all samples on the *m/z* 197 + 219 + 223 + 237 mass chromatograms (Fig. 7), albeit with large differences in relative abundance. In this paper, the ratio of Simonellite/1,3,6,7-TeMN was used to characterize the abundance of simonellite, and this parameter ranged from 2.85×10^{-3} to 46.1×10^{-3} with an average value of 12.0×10^{-3}.

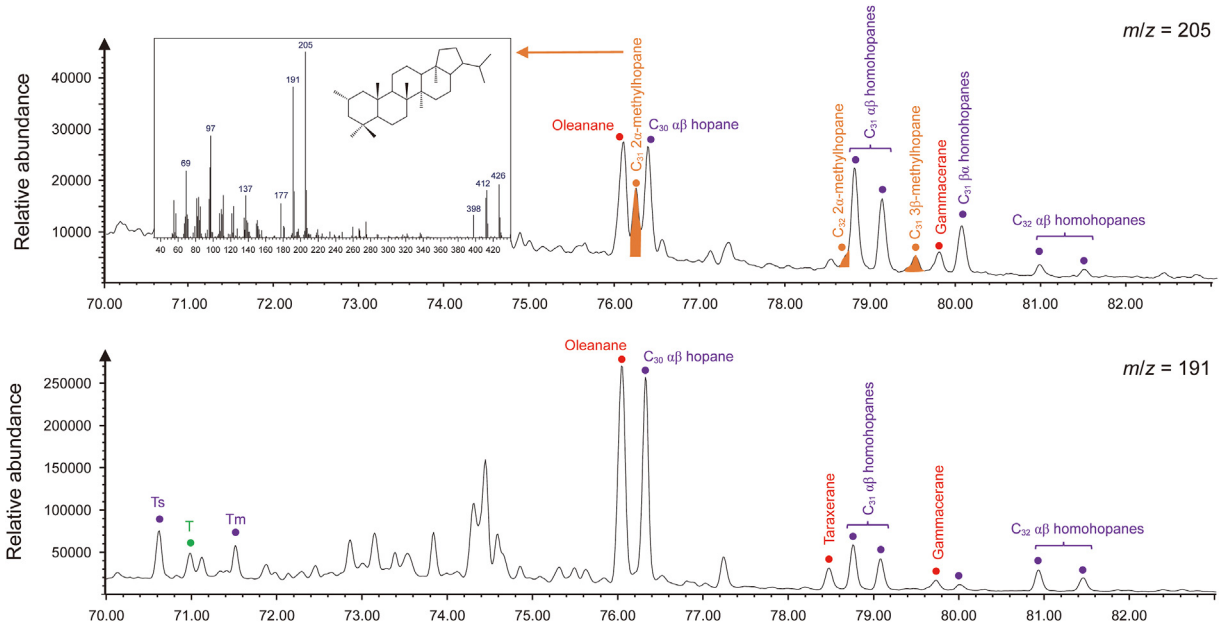

Fig. 3. Partial *m/z* 205 and *m/z* 191 mass chromatograms of sample L25-1 showing the distribution of methylhopane.

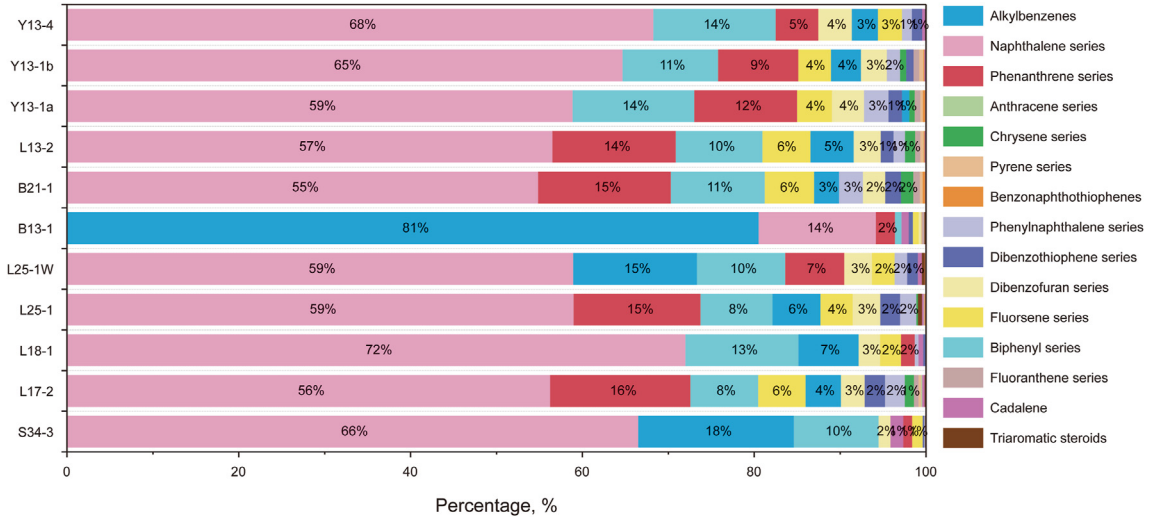

Fig. 4. Percentage bar chart showing the relative abundance of major aromatic hydrocarbon series. Relative abundance is based on peak areas in mass chromatograms. For example, the relative abundance of alkylbenzenes is defined as (alkylbenzenes/the sum of all aromatic compounds recognized) 100%.

4.5. Tetra- and hetero-aromatic compounds

The tetra-aromatic compounds were mainly composed of fluoranthrene, pyrene, chrysene, benzo[a]anthracene, benzo[b]anthracene, and benzonaphthothiophene and their alkyl derivatives (Fig. 6(c)), their contents were relatively low. The pyrene series mainly included pyrene and methylpyrene, with relative contents ranged from 0.01% to 0.99%. The abundances of the chrysene series ranged from 0 to 1.59%. The peak benzo[a]anthracene and benzo[b]anthracene was relatively low compared with chrysene on *m/z* 228 mass chromatogram (Fig. 6(c)).

Heterocyclic aromatic compounds mainly comprised DBT, DBF, and their alkylated homologues. The mean content of DBF series reach to 2.85%. The DBT series exhibited a distribution ranging from 0.21% to 2.34%, with a mean value of 1.31%. The paleoenvironmental proxy DBT/P was relatively low with a narrow distribution ranging from 0.11 to 0.34. The DBTs/DBFs ratios ranged from 0.13 to 1.67.

5. Discussions

5.1. Thermal alteration of the unusual sample B13-1

The crude oil B13-1 from the Songdong Sag appears to be unique, with significant differences in geological and geochemical characteristics compared with other samples. The low sterane isomerization extent (Fig. 8(b)) indicates its “low maturity” stage as previously reported (Huang et al., 2015), but neither crude oil property nor multiple molecular marker characteristics support this conclusion. At first, the significantly lower crude oil density (0.7151 g/cm^3) appears inconsistent with the characteristics of low maturity oil. Secondly, the exceedingly high content of short-chain alkylbenzenes (Fig. 8(a)) seems to be a characteristic of over-

Table 3
Aromatic biomarker parameters of crude oils in the Qiongdongnan basin.

Name	S34-3	L17-2	L18-1	L25-1	L25-1W	B13-1	B21-1	L13-2	Y13-1a	Y13-1b	Y13-4
Alkylbenzenes, %	18.18	4.22	7.13	5.66	14.38	80.48	3.03	5.13	1.01	3.61	3.22
N series, %	66.18	55.63	71.76	58.43	58.18	13.61	54.01	55.99	58.23	64.08	68.07
P series, %	1.20	16.13	1.76	14.59	6.94	2.22	15.22	14.22	12.00	9.38	5.11
Bip series, %	9.68	7.64	12.95	8.17	10.02	0.76	10.59	9.82	13.83	10.89	14.02
Trp series, %	0.007	0.151	0.031	0.127	0.119	0.006	0.288	0.090	0.334	0.093	0.117
PhN series, %	0.15	2.27	0.44	1.89	1.61	0.10	2.71	1.34	2.97	1.52	1.31
F series, %	1.05	5.46	2.24	3.57	2.45	0.53	5.64	5.53	3.84	3.61	2.63
DBT series, %	0.21	2.34	0.36	2.28	1.20	0.62	1.81	1.45	1.38	0.83	1.19
DBF series, %	1.52	2.56	2.51	3.16	3.19	0.28	2.40	2.97	3.69	2.83	3.71
Cadalene, %	1.34	0.13	0.38	0.18	0.48	0.69	0.02	0.06	0.03	0.10	0.15
TAS, %	0.01	0.08	0.00	0.28	0.17	0.04	0.00	0.00	0.00	0.00	0.01
Chrysene series, %	0.00	1.21	0.00	0.35	0.08	0.16	1.59	1.34	0.61	0.86	0.01
Pyrene series, %	0.02	0.35	0.01	0.09	0.04	0.14	0.50	0.37	0.48	0.48	0.03
Fluoranthene series, %	0.02	0.36	0.01	0.13	0.01	0.14	0.58	0.43	0.49	0.50	0.03
(N + Bip + F + Trp + PhN), %	77.07	71.08	87.39	72.38	72.42	–	72.96	72.69	78.88	80.10	86.04
(P + TAS), %	1.20	16.21	1.77	14.88	7.11	–	15.22	14.22	12.00	9.38	5.12
Simonellite/1,3,6,7-TeMN	46.1×10^{-3}	9.9×10^{-3}	15×10^{-3}	12.6×10^{-3}	8.8×10^{-3}	10.1×10^{-3}	5.9×10^{-3}	5.8×10^{-3}	5.8×10^{-3}	9.7×10^{-3}	2.8×10^{-3}
Cad/MDBTs	26.69	0.24	3.75	0.26	1.34	4.31	0.03	0.12	0.06	0.34	0.66
1,2,7-/1,3,7-TMN	0.38	0.46	0.31	0.31	0.44	0.43	0.42	0.65	0.28	0.32	0.38
DBT/P	0.19	0.22	0.28	0.21	0.21	0.18	0.11	0.12	0.16	0.13	0.34
DBTs/DBFs	0.13	0.85	0.13	0.62	0.32	1.67	0.66	0.41	0.36	0.27	0.31
Fla/(Fla + Py)	0.59	0.37	0.40	0.33	0.41	0.24	0.35	0.28	0.49	0.46	0.51
B[a]An/(B[a]An + Ch)	0.31	0.16	0.20	0.04	0.14	0.20	0.03	0.16	0.20	0.25	0.30
MPI	0.40	0.54	0.82	0.64	0.65	1.11	0.67	0.80	0.54	0.72	0.32
Type	A	B	B	B	B	–	C	C	D	D	D

MPI = 1.5 × (2−MP+3−MP)/(P+1 MP+9 MP), a commonly maturity indicator (Radke et al., 1982). The abbreviations see Appendix A.

mature crude oil (Lis et al., 2008; Tian et al., 2018). Furthermore, the absence of higher molecular weight n-alkanes distribution pattern suggests that crude oil B13-1 has undergone cracking, the equal Ro may be higher than 1.8% (Hill et al., 2003).

Evidence from secondary brine inclusion may provide new insights into the peculiar characteristics of B13-1. As is shown in Fig. 8(c), the reservoir of B13-1 underwent two orders of high-temperature fluid invasion, with the homogeneous temperature of the second order exceeding 210 °C, at which most of the saturated hydrocarbon biomarkers would be essentially destroyed. In fact, the biomarkers in crude oils may not always be derived directly from major source rocks but may be acquired during migration or after accumulation in the reservoir (Philp and Gilbert, 1982). The immature to low-mature shales of the underlying Meishan Formation may be responsible for the "low maturity" steranes and terpanes, as their saturated hydrocarbon biomarker signatures are highly consistent with crude oil B13-1 (Liang et al., 2015). We propose that B13-1 is a unique sample that may have suffered from thermal alteration, causing its biomarkers to be unable to fully reflect the original geological characteristics.

5.2. Depositional environment of related source rocks

Isoprenoid alkanes DBTs, DBFs and homohopanes are environmentally-sensitive biomarkers, with many useful plates having been developed by predecessors (Hughes et al., 1995; Radke et al., 2000; Li et al., 2013). Pr/Ph ratio is a commonly used redox proxy, greater than 3.0 reflects a suboxic to oxic condition (Peters et al., 2005). Heterocyclic compounds were closely related to the organic facies and depositional environment of sediments and oils, they were the result of a surface reactions of compounds with biphenyl structures (Asif et al., 2009, 2010). The abundance of DBF and its homologues were more relevant to marine environment, whereas dibenzofuran and its homologues were oxic environment (Fan et al., 1991; Asif and Wenger, 2019).

Fig. 9(a)–(c) show that the crude oils in the Qiongdongnan Basin originate from terrestrial Type III source rock and influenced by a fluvial-delta depositional system, which also indicating a significant contribution from higher plants. The Pr/Ph ratios of crude oil samples are generally greater than 3.0, while the DBTs/DBFs ratios are predominantly below 1.0. These characteristics suggest that crude oils in the Qiongdongnan Basin are mainly generated from source rocks deposited under oxic conditions.

C_{31} to C_{35} homohopanes are considered to originate from bacteria, and their contents also reflect the redox conditions (Connan et al., 1986). Coaly type III source rocks deposited under oxic conditions yield oils usually with low C_{32}–C_{35} homohopanes (Peters and Moldowan, 1991). It is worth mentioning that the oil samples from the Central Depression (Types B and C) have relatively higher C_{32}–C_{35} homohopanes/C_{30}H ratios. This suggests that the related source rocks in the Central Depression deposited under more reducing condition. The detection of methylhopanes can also provide new insights into the water column environment of the Central Depression during Oligocene.

2-methylhopane derived from bacteriohopanepolyols (BHPs) are normally regarded as an indicator of photosynthetic cyanobacteria extensively host in marine settings, and they are also used as an indicator of depositional environment in petroleum system, and typically enrichment in the lower suboxic zone of stratified water column (Summons et al., 1999; Wang et al., 2006; Blumenberg et al., 2013; Kharbush et al., 2018; Elling et al., 2021). BHPs seem to be faithful recorders of enclosed and oxygen-deficient water column (Kusch and Rush, 2022). The identification of 2α-methylhopane in crude oils from the Central Depression indicates an enclosed and quiet water column during the deposition of corresponding source rocks, in consistent with the evolutions of sedimentary facies (Liu et al., 2023). The extremely low abundance of C_{32}–C_{35} 2-methylhopanes in the crude oils may suggest subanoxic–suboxic conditions rather than oxic in the Central Depression during Oligocene (Fig. 3).

5.3. Evidence of gymnosperm input from aromatic compounds

The sources of PAHs in ancient sediments and crude oils mainly

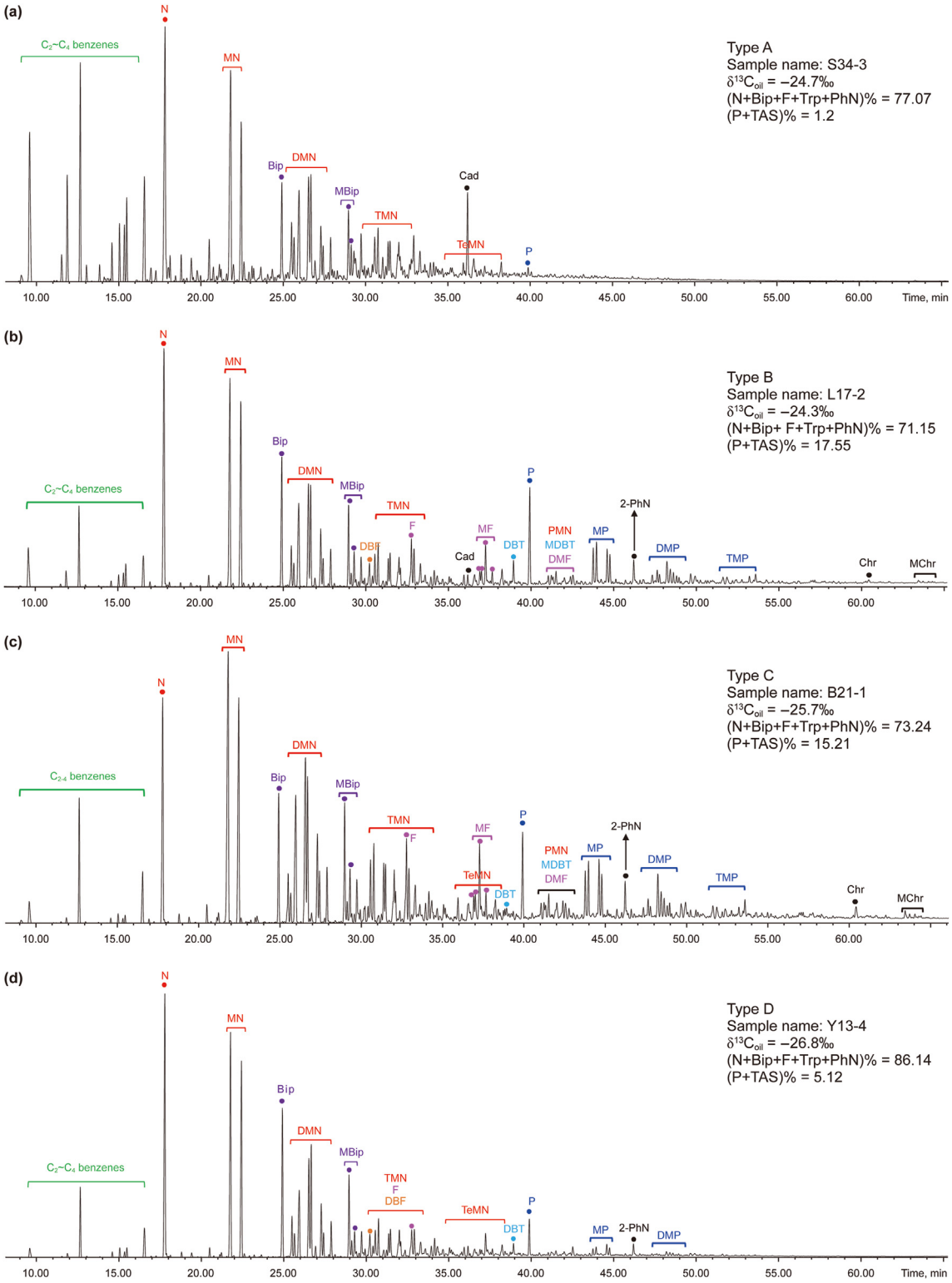

Fig. 5. Total ion chromatogram (TIC) of the aromatic hydrocarbons in four representative crude oils. The abbreviations of compounds see Appendix A.

include wildfire combustion and the burial diagenesis of biological debris. PAHs from wildfires are typically characterized by high abundance of non-substituted fluoranthene, pyrene, benzo[a]fluoranthene, benzo[e]pyrene benzo[a]pyrene, perylene, benzo[ghi] perylene and coronene (Laflamme and Hites, 1978; Killops and Massoud, 1992; Jiang et al., 1998). PAHs from combustion have been reported in Miocene sediments of the Yinggehai basin (Ding et al., 2022). The burial diagenesis and wildfire combustion origin can be distinguished by cross plot of Fla/(Fla + Py) to B[a]An/(B[a]An + Ch) (Yunker et al., 2002).

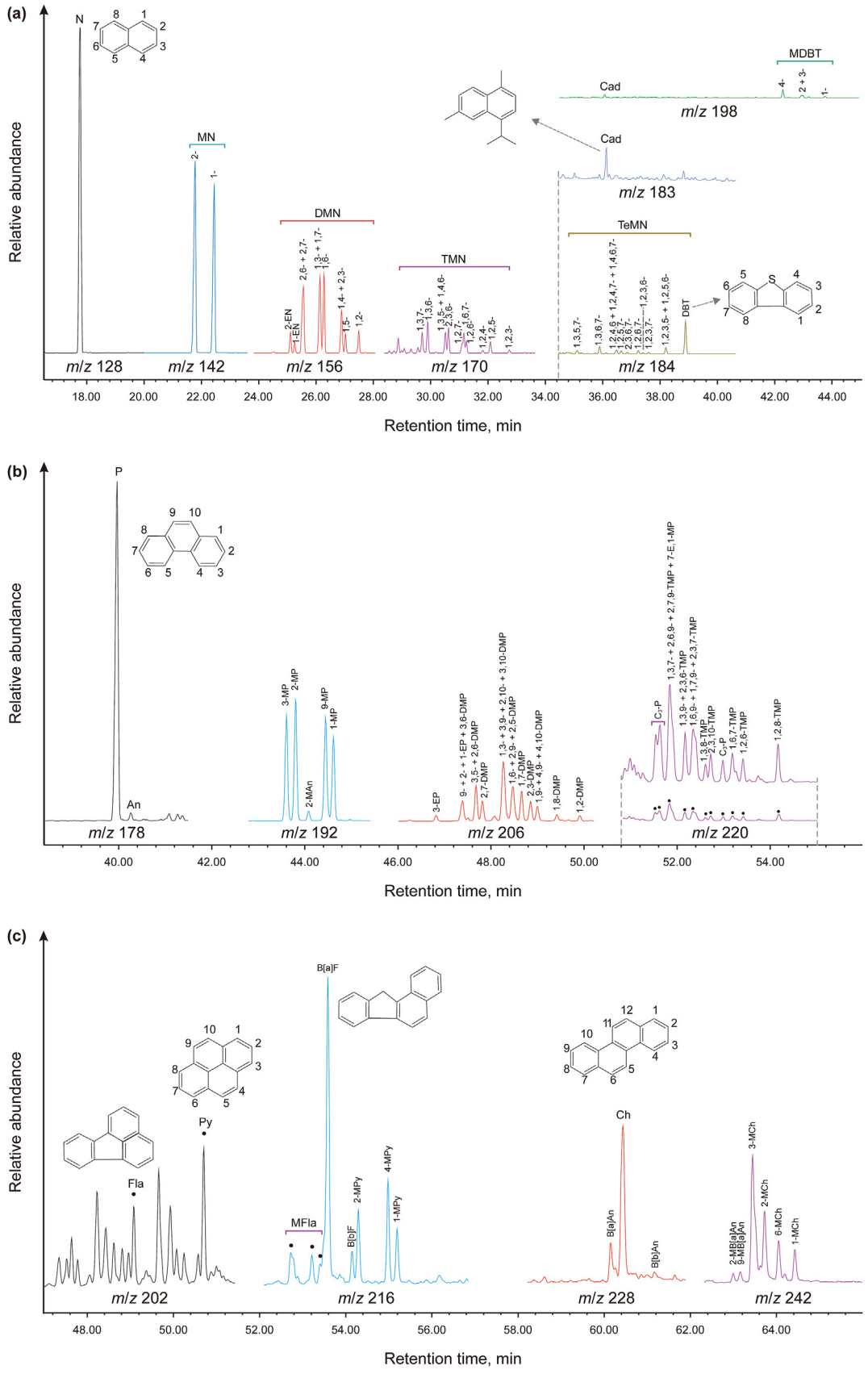

Fig. 6. Partial mass chromatograms of **(a)** *m/z* 128 + 142 + 156 + 170 + 184 + 198, **(b)** *m/z* 178 + 198 + 206 + 220, and **(c)** *m/z* 202 + 216 + 228 + 242 of the representative sample L17-2. The abbreviations of compounds are shown in Appendix A.

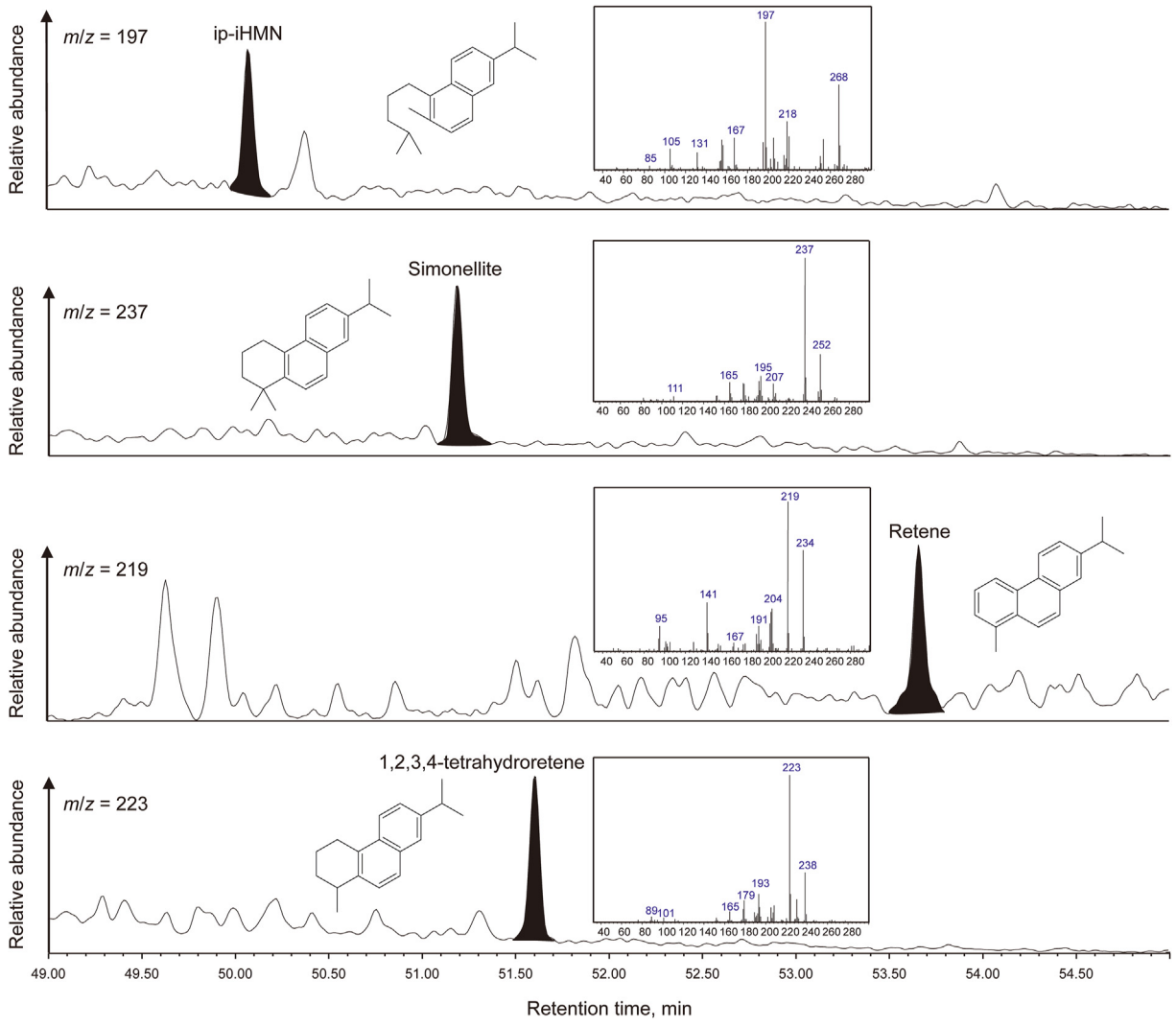

Fig. 7. Partial mass chromatograms showing the identification of ip-iHMN (*m/z* 197), simonellite (*m/z* 237), retene (*m/z* 219), and 1,2,3,4-tetrahydroretene in sample S34-3.

According to Fig. 10(a), PAHs in most crude oils primarily derive from the burial diagenesis of biomass. A slight contribution of PAHs from combustion sources was distinguished in sample S34-3, Y13-1a, Y13-1b, and Y13-4. Since prominently unsubstituted PAHs are not observed in the TICs of aromatic fractions, we believe that combustion sources play a minor role in crude oils, with the primary source being the diagenetic evolution of deposited organic matter.

The prevalence of oleanane and bicadinane in most crude oils reflected the important contribution of angiosperms in the Qiongdongnan Basin (Zhou et al., 2003). Surprisingly, high abundances of simonellite, retene, 1,2,3,4-tetrahydroretene, ip-iHMN, and cadalene were detected in the aromatic fraction of sample S34-3. Both cadalene and simonellite are recognized as indicators of terrestrial higher plants, of which simonellite is more specific to coniferous gymnosperms (Simoneit et al., 1986; Püttmann and Villar, 1987; Alexander et al., 1988; Ellis et al., 1995). Cad/MDBTs ratio shows a significant positive correlation with Simonellite/1,3,6,7-TeMN ($R^2 = 0.95$) (Fig. 10(b)), but exhibits a negative correlation with (W + T + R)/C_{30}H (Fig. 10(c)) and no obvious correlation with Oleanane/C_{30}H (Fig. 10(d)). The extremely low content of oleanane and bicadinanes indicates a low contribution of angiosperms to sample S34-3 (Fig. 2). It should be noted that the higher thermal stability of aromatic biomarkers (cadalene and simonellite) than saturated biomarkers (oleanane and bicadinane) may lead to an overestimation of the gymnosperm contribution. The crude oils in our study (excluding B13-1 due to its thermal alteration in the reservoir) are mainly generated during oil window (Zhou et al., 2003; Xu et al., 2023a), as evidenced by the sterane isomerization parameter C_{29} S/(S + R) in Table 2, which also indicates the mature stage of this crude oils. However, there is no positive correlation between C_{29} S/(S + R) with Cad/MDBTs and Simonellite/1,3,6,7-TeMN. Although maturity has theoretically effects on the contents of these biological source indicators, we suggest that the input of biological sources is the dominant factor in the Qiongdongnan Basin. This viewpoint was also reported in the northwest margin of Australia (van Aarssen et al., 2000). Furthermore, the absence of aromatized oleananes in all crude oils reveals a low aromatization level of oleanane-type triterpanes. These features suggest that the cadalene in the Qiongdongnan Basin seems to be mainly derived from coniferous gymnosperms rather than angiosperms. The outstanding gymnosperms-derived biomarkers imply a higher contribution of gymnosperms to crude oil S34-3 than other crude oils.

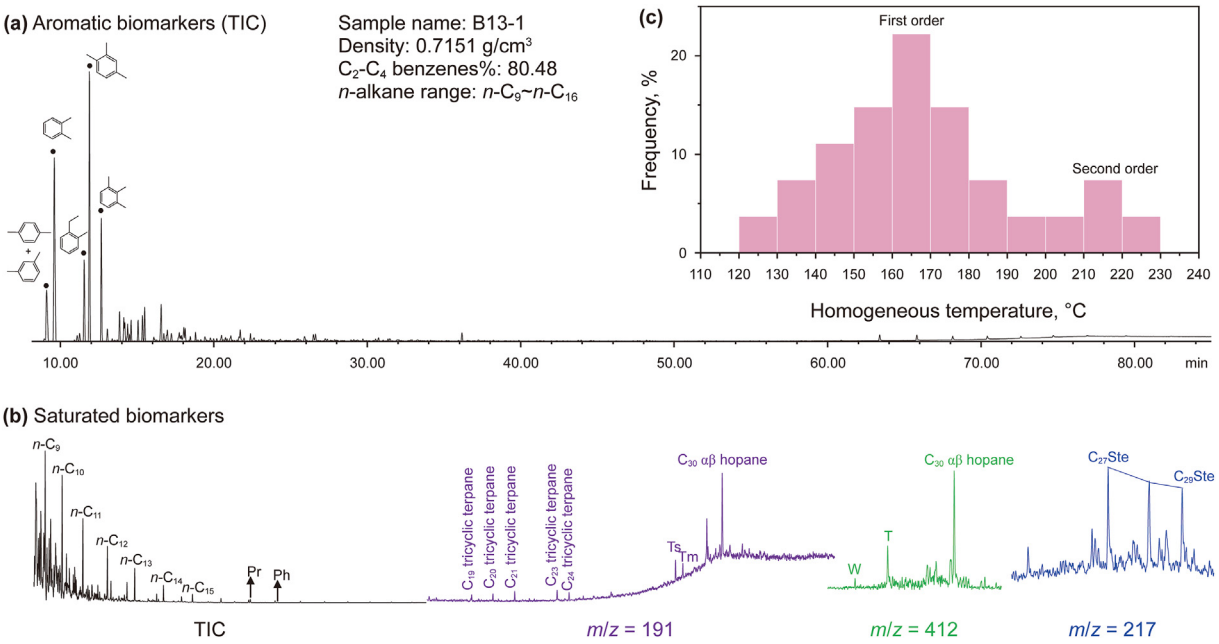

Fig. 8. **(a)** The TIC of the aromatic fraction of crude oil B13-1. **(b)** The biomarker fingerprints of the saturated fraction of crude oil B13-1. **(c)** The homogeneous temperature distribution of secondary brine inclusions in the reservoir (Meishan Formation, 1577–1580 m) where crude oil B13-1 is located.

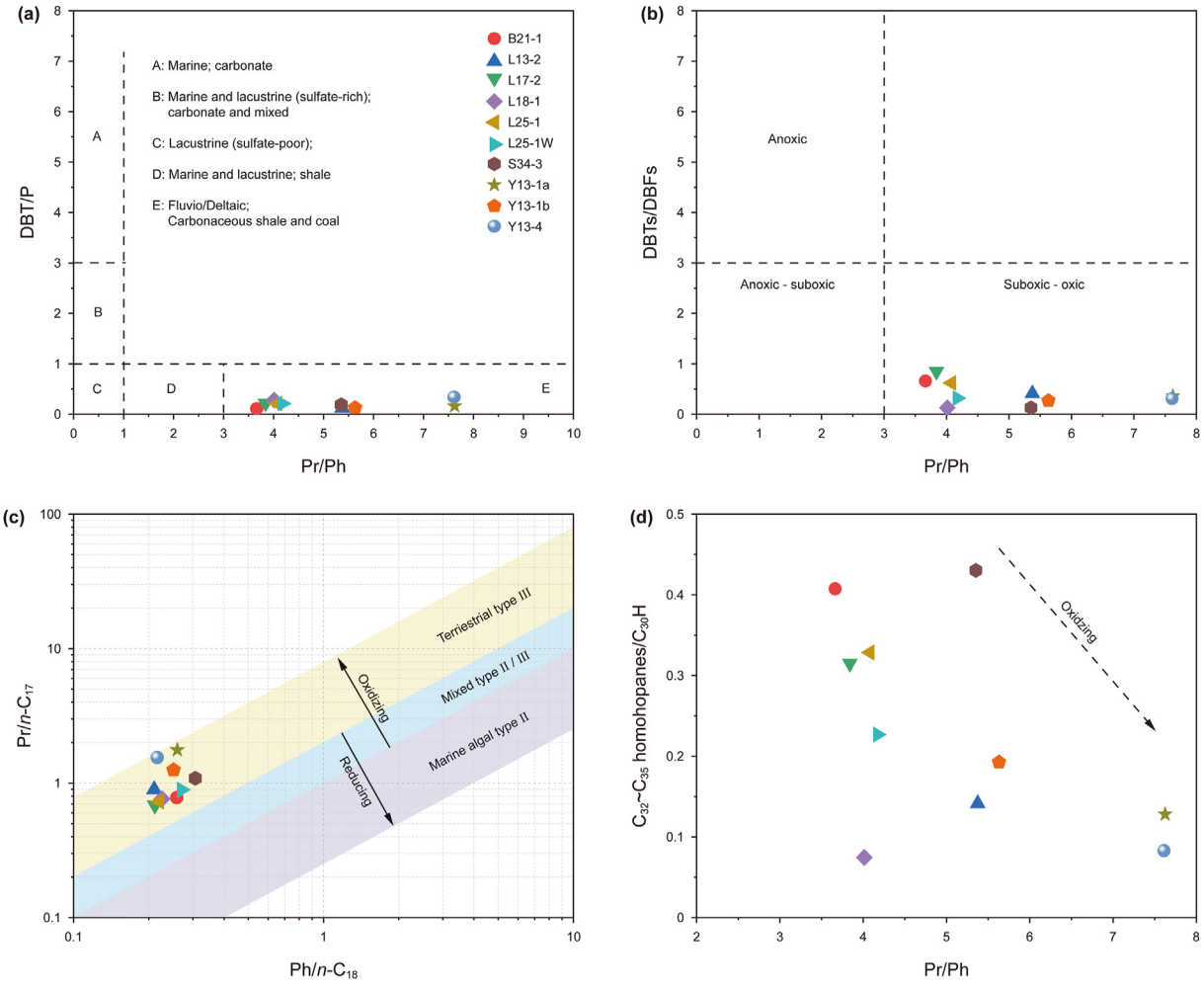

Fig. 9. Scatter plots of biomarker parameters related to depositional environment.

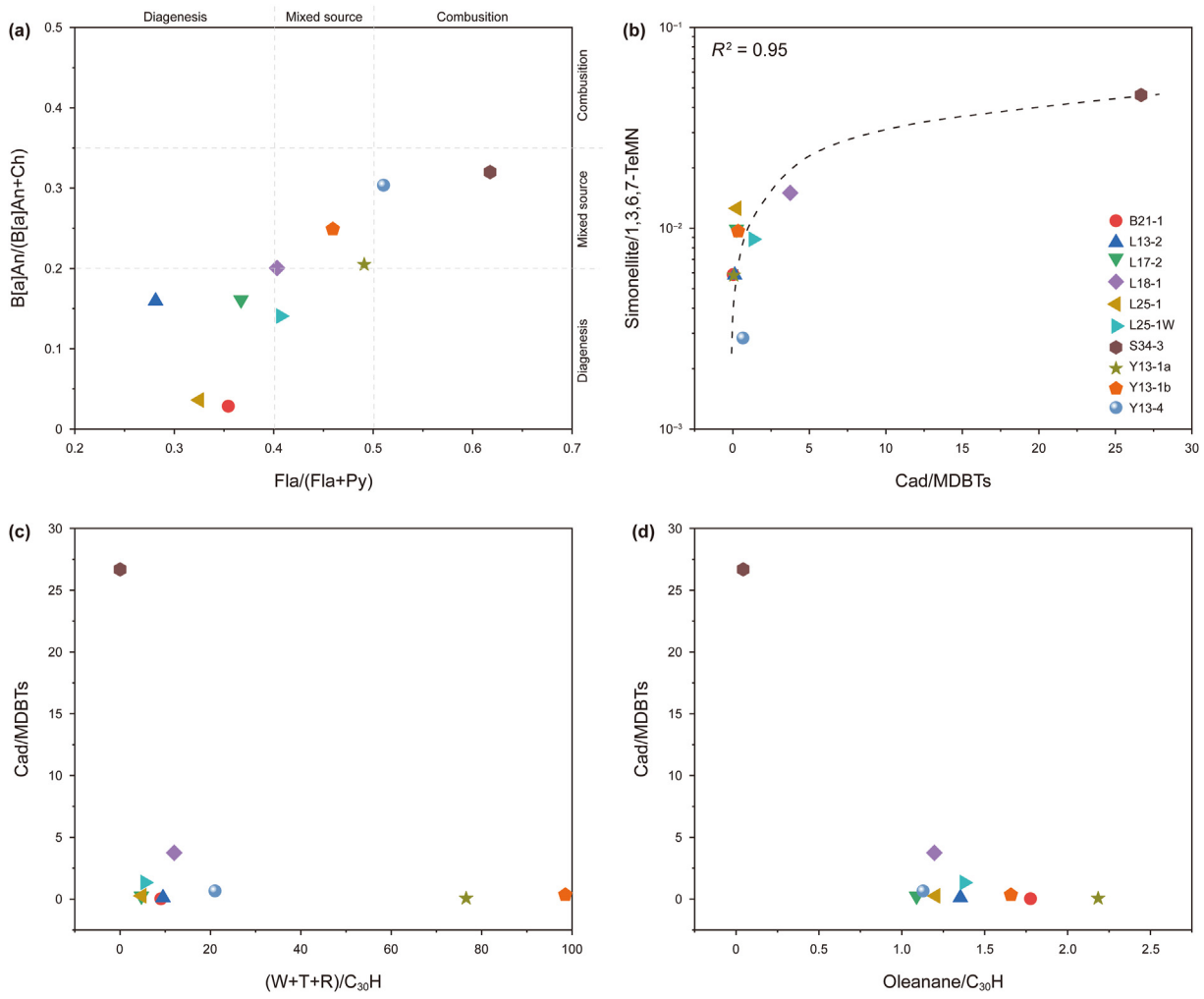

Fig. 10. PAHs cross plot for the ratios of **(a)** Fla/(Fla + Py) and B[a]An/(B[a]An + Ch), **(b)** Cad/MDBTs and Simonellite/1,3,6,7-TeMN, **(c)** (W + R + T)/C_{30}H and Cad/MDBTs, **(d)** Oleanane/C_{30}H and Cad/MDBTs. The abbreviations of compounds see the notes of Table 2 and Appendix A.

5.4. Biological source composition of oils

In the past, assessments of the biogenic origin of hydrocarbons in the Qiongdongnan Basin were primarily based on the composition of saturated hydrocarbon biomarkers (Zhou et al., 2003; Xiao et al., 2006). The high abundances of oleanane, des-A-oleanane and its derivatives (compounds X, Y, and Z in Fig. 2), rearranged oleanane (compounds I, II, and III in Fig. 2), bicadinanes, and taraxerane naturally supported the significant contribution of angiosperms to crude oils in the Qiongdongnan Basin. However, there are still many contradictions cannot be explained reasonably by saturated hydrocarbon biomarkers, such as the conflict between the high abundance of oleanane and bicadinanes with high C_{27} regular steranes in sample L18-1 (Table 2). The $\delta^{13}C_{oil}$ is mainly determined by the composition of the source material, with little impact from maturation, making it a potential indicator for source assessment (Hayes et al., 1987; Schoell et al., 1994).

We screened 14 biological source proxies, attempting to establish their correlation with the $\delta^{13}C_{oil}$. Pr/Ph, C_{19}TT/C_{30}H, Oleanane/C_{30}H, Taraxerane/C_{30}H, (W + T + R)/C_{30}H, C_{29} regular steranes%, and 1,2,7-/1,3,7-TMN are commonly employed as indicators of terrigenous organic matter. A high Pr/Ph ratio typically reflects the input of terrigenous organic matter under oxidizing conditions (Sofer, 1984). Oleanane indicates the contribution of angiosperms after the Cretaceous (Moldowan et al., 1994). The high abundance of C_{19} and C_{20} tricyclicterpanes originates from vascular plants (Barnes and Barnes, 1983). Taraxerane shares a similar origin with oleanane, but a high abundance of taraxerane usually indicate the input of mangrove vegetation (Versteegh et al., 2004). Bicadinanes are believed to originate from the Dipterocarpaceae family of angiosperms (van Aarssen et al., 1990). C_{29} regular steranes are generally associated with higher plants, but cyanobacteria and brown algae can also synthesize their precursors (Huang and Meinschein, 1979; Moldowan et al., 1985; Volkman, 1986). The 1,2,7-TMN appears to be derived directly from the degradation of oleanane-type triterpenoids in angiosperms (Strachan et al., 1988).

In contrast, C_{23}TT/C_{30}H, Gammacerane/C_{30}H, 2α-methylhopane/C_{30}H and C_{27} regular steranes% were screened as indicators of marine organic matter. C_{23} tricyclicterpane is the typically dominant compound in tricyclicterpanes of marine crude oils, associated with Tasmanian algae (Azevedo et al., 1992). Gammacerane is an effective biomarker of water stratification and salinity (Damsté et al., 1995), and a certain level of water salinity was conducive to the growth of marine algae (Wu et al., 2018). C_{27} regular steranes originate from marine sources and are highly abundant in rhodophyta (Summons et al., 1988; Kodner et al., 2008). The enclosed and oxygen-deficient environment revealed by 2α-methylhopane supports both algal growth and preservation (Wójcik-Tabol et al.,

2022). Simonellite has been suggested to be the diagenetic products of abietic acid type compounds from conifer resins (Simoneit et al., 1986; van Aarssen et al., 2000). Phenanthrene and the triaromatic sterane series are more closely associated with lower aquatic organisms (Riolo et al., 1986; George, 1992; Radke and Willsch, 1993; Budzinsky et al., 1995), while naphthalene, biphenyl, fluorene, triphenyl, and phenylnaphthalene series are more closely related to higher plants. The percentages of (P + TAS) series and (N + Bip + F + Trp + PhN) series to all aromatic compounds were proposed to reflect the contributions of marine and terrestrial sources in this paper, respectively.

We performed Spearman correlation analysis on the above 14 direct/indirect source proxies with $\delta^{13}C_{oil}$. As shown in Figs. 11 and 12, the majority of terrestrial source proxies, including Pr/Ph, $C_{19}TT/C_{30}H$, Taraxerane/$C_{30}H$, (W + T + R)/$C_{30}H$, and (N + Bip + F + Trp + PhN)% exhibit good negative correlations with the $\delta^{13}C_{oil}$. The weak correlation between Oleanane/$C_{30}H$, 1,2,7-/1,3,7-TMN and $\delta^{13}C_{oil}$ is disappointing. Precisely, the high abundance of oleanane in crude oils can only confirm the contribution of angiosperms, there is no quantitative relationship between them. This is because the contact of plant matter with seawater during early diagenesis enhances the expression of oleananes in mature sediment or oil (Murray et al., 1997). On the contrary, the correlations between marine source proxies and carbon isotopes varies significantly (Fig. 11), the commonly used indicators of marine algae, such as C_{27} regular steranes% and $C_{23}TT/C_{30}H$, show no and negative correlation with the $\delta^{13}C_{oil}$. We speculate that and the content of C_{27} regular streranes or C_{23} tricyclicterpane cannot fully characterize the overall contribution of marine algae. Similarly, multiple sources of C_{29} steranes may account for the weak correlation between C_{29} regular steranes% with the $\delta^{13}C_{oil}$. There is a certain positive correlation between Gammacerane/$C_{30}H$, 2α-methylhopane/$C_{30}H$, and (P + TAS) % with $\delta^{13}C_{oil}$ (Figs. 11 and 13(a)–(c)). This is because Gammacerane/$C_{30}H$, 2α-methylhopane/$C_{30}H$, and (P + TAS)% proxies reflect the overall marine algae contribution, whereas C_{27} regular steranes% and $C_{23}TT/C_{30}H$ represent the different algae taxa (Summons et al., 1988; Azevedo et al., 1992).

Spearman correlation analysis of multiple source proxies reveals that crude oils originating from terrestrial organic matter tend to exhibit relatively lighter whole oil isotopes, whereas those generated by marine organic matter tend to have heavier isotopes. This phenomenon has also been observed in the oil-source correlations of the Qiongdongnan Basin and Yinggehai Basin (Zhu et al., 2018). It should be noted that the differences in carbon sources of photosynthesis results in the carbon isotope difference of marine and terrigenous organic matter (Galimov, 2006; Lamb et al., 2006). Terrestrial higher plants directly absorb atmospheric CO_2, while marine algae utilize the isotopically heavier HCO_3^- in column water (Schidlowski et al., 1984; Kump and Arthur, 1999; Mackensen and Schmiedl, 2019).

Both terrestrial higher plants and marine algae are considered to be the primary biological sources of crude oils in the Qiongdongnan Basin, but varies regionally. Based on the $\delta^{13}C_{oil}$ and molecular biomarker signatures, we divided these oils (excluding B13-1) into four types and summarized their biological source compositions.

Type A crude oils (solely sample S34-3) are characterized by a high Pr/Ph ratio, C_{29} regular sterane, terrestrial aromatic compounds, and an extremely low level of angiosperm-derived compounds (Figs. 2 and 5), indicating a biological source of mainly non-angiosperm plants. Remarkable simonellite and cadalene suggest an increased contribution from conifer gymnosperms compared with other samples (Fig. 13(d)), which is also consistent with its heavy $\delta^{13}C_{oil}$ (−24.7‰), as conifer gymnosperms typically

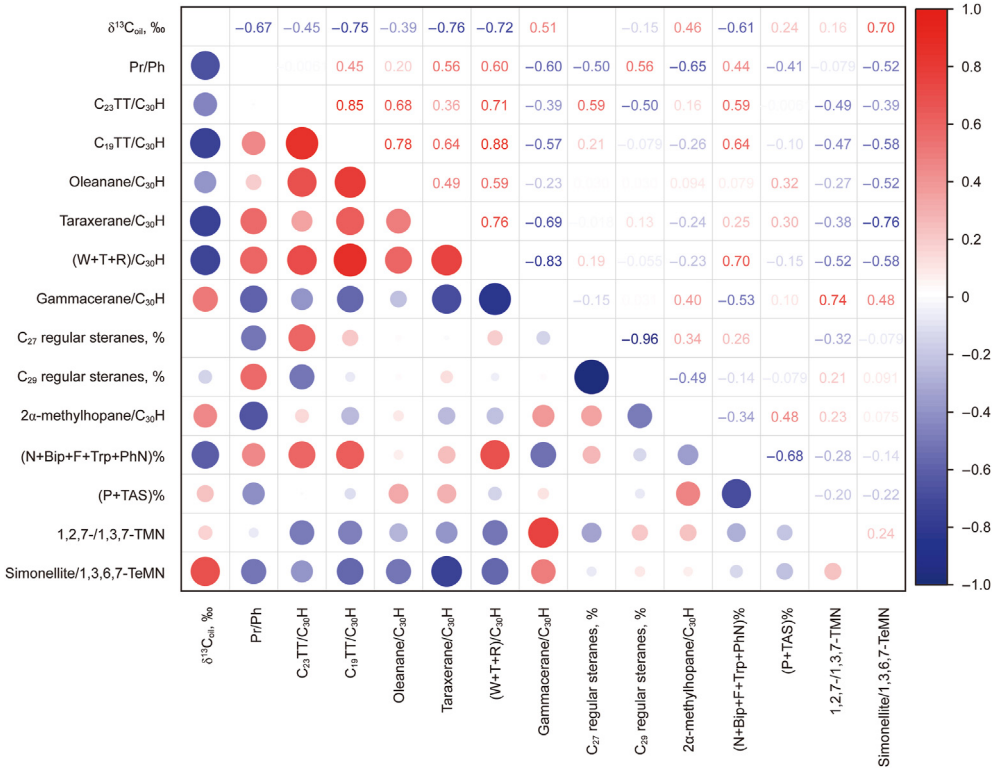

Fig. 11. The heat map of Spearman correlation coefficient matrix for geochemical parameters crude oils (excluding B13-1). Blue circles represent negative correlations, red circles represent positive correlations, and the size of the circles indicates the strength of the correlation). Absolute correlation coefficients greater than 0.6 indicate a strong correlation, while coefficients within the range of 0–0.2 suggest no or weak correlation.

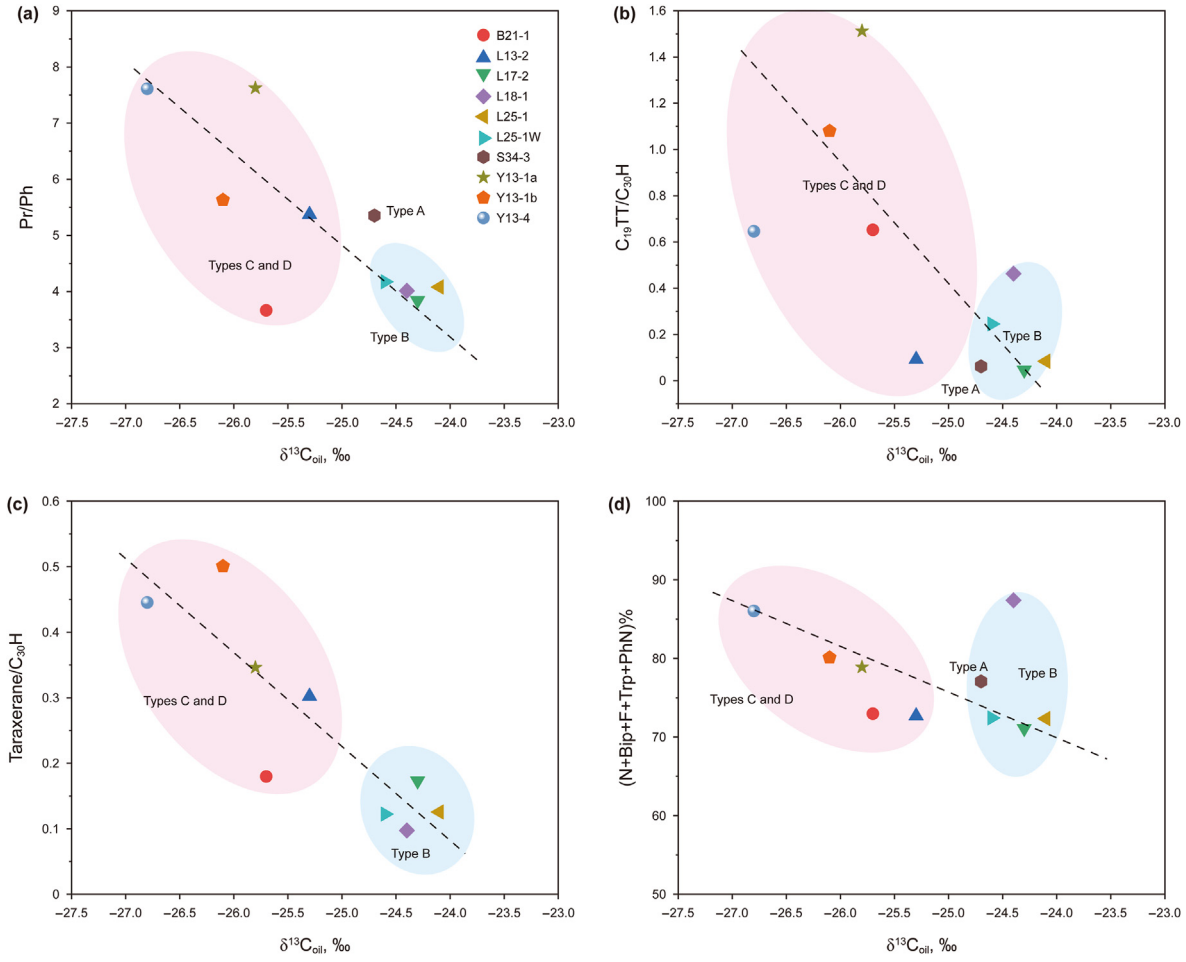

Fig. 12. Correlation plots of Pr/Ph, $C_{19}TT/C_{30}H$, Taraxerane/$C_{30}H$, and (N + Bip + F + Trp + PhN)% to $\delta^{13}C_{oil}$.

isotopically heavier 2‰–2.5‰ than angiosperms during Oligocene (Murray et al., 1998; Karp et al., 2020; Richey et al., 2023). Furthermore, the previous researchers also observed an increase in the content of gymnosperm pollen in the third member of the Lingshui Formation shales (Ding et al., 2021) providing geological evidence for the contribution of gymnosperms. The low level of 4-methylsteranes indicates dinoflagellate sourcing from the Eocene lacustrine source rock, but significant differences between the kerogen carbon isotopes of lacustrine oil shale (approx. −28‰, unpublished data from a newly drilled well in the Songxi Sag) and the high $\delta^{13}C_{oil}$ values of crude oil S34-3 may suggest a minor contribution from dinoflagellates.

Type B crude oils (L17-2, L18-1, L25-1, and L25-1W) distributes in the western part of the Central depression, possess high oleanane, bicadinene, marine aromatic compounds, along with relatively low Pr/Ph, C_{19} tricyclicterpane, taraxerane and terrestrial aromatic compounds, reflecting a mixed biological source of mainly angiosperm plants and marine algae. The relatively heavy $\delta^{13}C_{oil}$ (−24‰ to −25‰) indicate the increasing contribution of marine algae. The contribution of marine algae to hydrocarbons in the Central Depression may have been long neglected in the past, as it is usually overshadowed by the significant features of angiosperm input. The latest research on tectonic and paleogeographic indicate that the sags in the Central Depression were independent with semi-enclosed water bodies during the early Oligocene, providing a geological foundation conducive to the development of marine algae (Liu et al., 2023; Xu et al., 2023a). The presence of marine algae in the Central Depression during the early Oligocene has been well described (Xu et al., 2023b). Additionally, the western part of the Central Depression is minimally influenced by deltas, and up to 39% marine dinophyceae spores were observed in some marine terrigenous source rocks (Xiong et al., 2019).

Type C crude oils (B21-1 and L13-2), also collected from the Central Depression, exhibit a collaborative contribution primarily from angiosperm plants and marine algae (Figs. 2 and 5). Overall, this type of crude oil shows similar characteristics of marine algal biomarkers as Type B (Fig. 13(a)–(c)), but higher Pr/Ph ratio, taraxerane, terrestrial aromatic compounds, C_{19} tricyclicterpane (Fig. 12), and lighter $\delta^{13}C_{oil}$ values (−25‰ to −26‰) may imply a predominant contribution of angiosperms.

Type D crude oils (Y13-1a, Y13-1b, and Y13-4, obtained from the shallow-water YC13 gas fields) are believed to be generated by coal measure source rock in the Yacheng formation (Xiao et al., 2006). They are distinguished by abnormally high angiosperm biomarkers and C_{19} tricyclicterpane, along with low algal molecular biomarkers and lightest $\delta^{13}C_{oil}$ (mainly below −26‰), reflecting the prime contribution of angiosperms. Furthermore, significant input of mangrove vegetation is revealed by the high taraxerane contents (Fig. 2).

6. Conclusions

Substantial molecular biomarkers are identified in crude oils from the Qiongdongdong Basin, providing novel insights into the

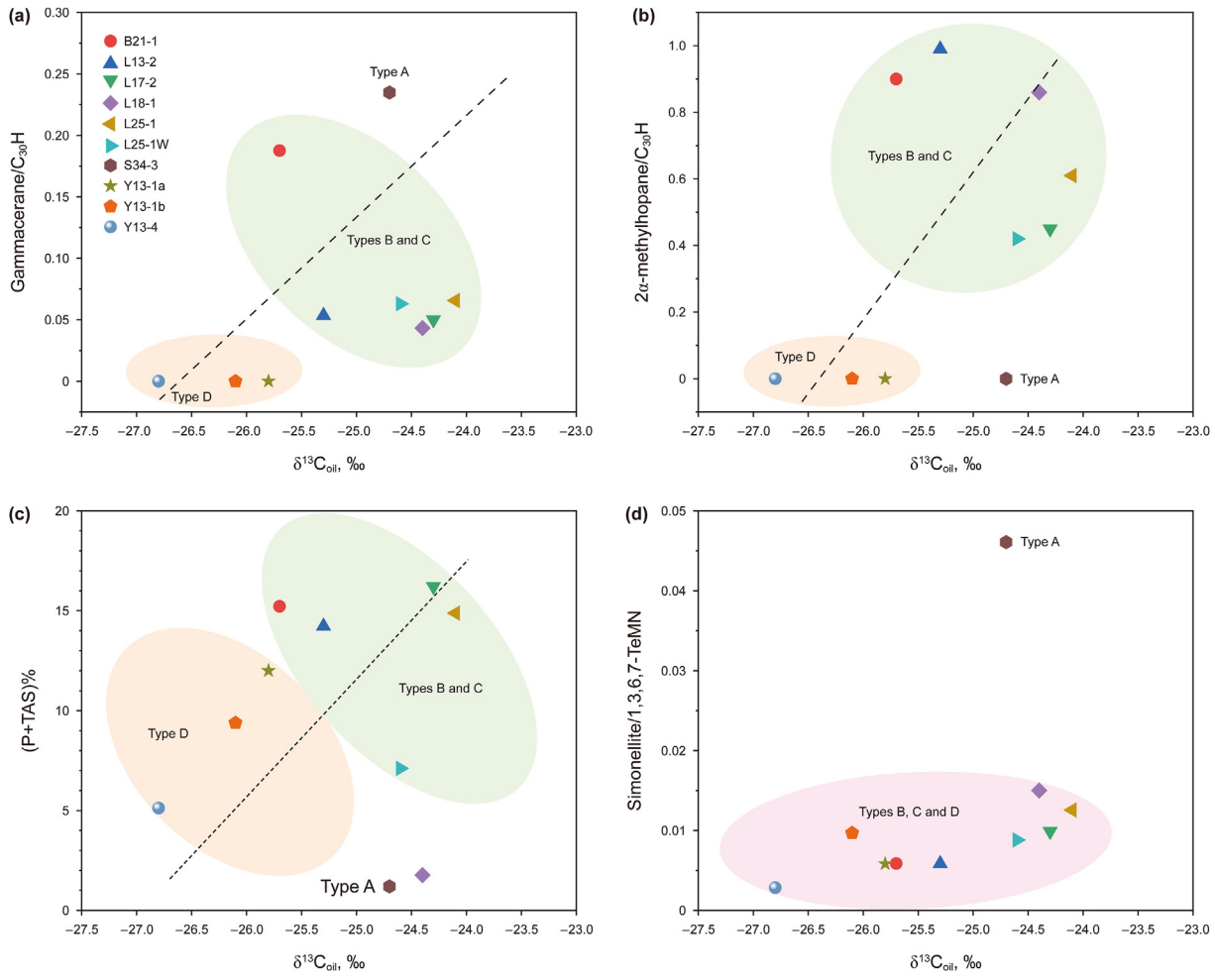

Fig. 13. Correlation plots of Gammacerane/C_{30}H, 2α-methylhopane/C_{30}H, (P + TAS)%, and Simonellite/1,3,6,7-TeMN to $\delta^{13}C_{oil}$.

organic matter input and depositional environment together with the whole oil carbon isotopes. The depositional environments in the Qiongdongnan Basin are mainly determined as oxic–suboxic, as indicated by isoprenoid alkanes, hetero-aromatic compounds and their homohopanes. The occurrence and distribution characteristics of 2-methylhopane in crude oils suggest an enclosed water column and subanoxic–suboxic condition in the Central Depression during early Oligocene.

Evidence from density, n-alkanes, short chain alkylbenzenes and secondary brine inclusions indicates that the unique crude oil B13–1 may have suffered from thermal alteration. High abundances of oleananes and bicadinanes in most crude oils demonstrate the significant contribution of angiosperms. However, the presence of simonellite and related compounds in sample S34-3 provides an evidence for the input of coniferous gymnosperms. Cadalene in aromatic fractions shows a no/negative correlation with angiosperm-derived compounds but a strong positive correlation with simonellite, suggesting a potential association with coniferous gymnosperms.

The crude oils in the Qiongdongnan Basin can be classified into four types using molecular biomarkers and the whole oil carbon isotopes. Type A oil is characterized by a terrestrial biological source, mainly consisting of non-angiosperm plants, with minor dinoflagellates and increasing contribution from conifer gymnosperms compared with other samples. The biological sources of Type B oils from the western part of the Central Depression are primarily angiosperm plants and marine algae, the relatively heavy $\delta^{13}C_{oil}$ (−24‰ to −25‰) and geological setting of their related source rocks suggesting the increasing contribution of marine algae. Type C oils share similar biological sources with type B, but the moderately $\delta^{13}C_{oil}$ (−25‰ to −26‰) and high level of terrestrial biomarkers indicating a predominant contribution of angiosperms. Type D oils possess the lightest isotopes, primarily sourced from angiosperms, with mangrove vegetation playing an important role. The whole oil carbon isotope appears to be one of the most reliable geochemical indicators for discriminating the sources of crude oils along with biomarkers in the Qiongdongnan Basin. The contribution of marine algae in the Central Depression may have been neglected in the past.

CRediT authorship contribution statement

Zi-Ming Zhang: Writing – original draft, Methodology, Investigation. **Du-Jie Hou:** Supervision, Resources. **Xiong Cheng:** Funding acquisition. **Da-Ye Chen:** Investigation. **Gang Liang:** Resources. **Xia-Ze Yan:** Data curation. **Wei-He Chen:** Conceptualization.

Declaration of competing interest

The authors declare that they have no known competing financial interests or personal relationships that could have appeared to influence the work reported in this paper.

Acknowledgements

This research was supported by the National Natural Science Foundation of China (Grant No. 42302189). Thanks to Lecturer Qi Chen (Yangtze University) for the guidance of experiments in this research particularly.

Appendix A. The abbreviation list of aromatic compounds mentioned in the text.

m/z	Compounds	Abbreviation	*m/z*	Compounds	Abbreviation
128	Naphthalene	N	198	Methyldibenzothiophene	MDBT
142	Methylnaphthalene	MN	168	Dibenzofuran	DBF
156	Ethylnaphthalene	EN	182	Methyldibenzofuran	MDBF
156	Dimethylnaphthalene	DMN	197	6-isopro-pyl-1-isohexyl-2-methylnaphthalene	ip-iHMN
170	Trimethylnaphthalene	TMN	198	Cadalene	Cad
184	Tetramethylnaphthalene	TeMN	204	Phenylnaphthalene	PhN
198	Pentamethylnaphthalene	PMN	234	Benzonaphthothiophene	BNT
178	Phenanthrene	P	202	Fluoranthene	Fla
192	Methylphenanthrene	MP	216	Methylfluoranthene	MFla
206	Dimethylphenanthrene	DMP	216	Benzo[a]fluorene	B[a]F
206	Ethylphenanthrene	EP	216	Benzo[b]fluorene	B[b]F
220	Trimethylphenanthrene	TMP	202	Pyrene	Py
178	Anthracene	An	216	Methylpyrene	MPy
192	Methylanthracene	MAn	228	Chrysene	Ch
154	Biphenyl	Bip	242	Methylchrysene	MCh
168	Methylbiphenyl	MBip	228	Benzo[a]anthracene	B[a]An
166	Fluorsene	F	228	Benzo[b]anthracene	B[b]An
180	Methylfluorsene	MF	242	Methylbenzo[a]anthracene	MB[a]An
194	Dimethylfluorsene	DMF	230	Triphenyl	Trp
184	Dibenzothiophene	DBT	231	Triaromatic steroid	TAS

Supplementary data

Supplementary data to this article can be found online at https://doi.org/10.1016/j.petsci.2024.05.026.

References

Alexander, R., Kagi, R.I., Toh, E., et al., 1988. The use of plant-derived biomarkers for correlation of oils with source rocks in the Cooper/Eromanga Basin system. Aust. Pet. Explor. Assoc. J. 28, 310–324. https://doi.org/10.1071/aj87024.

Asif, M., Alexander, R., Fazeelat, T., et al., 2010. Sedimentary processes for the geosynthesis of heterocyclic aromatic hydrocarbons and fluorenes by surface reactions. Org. Geochem. 41, 522–530. https://doi.org/10.1016/j.orggeochem.2009.12.002.

Asif, M., Alexander, R., Fazeelat, T., et al., 2009. Geosynthesis of dibenzothiophene and alkyl dibenzothiophenes in crude oils and sediments by carbon catalysis. Org. Geochem. 40, 895–901. https://doi.org/10.1016/j.orggeochem.2009.04.016.

Asif, M., Wenger, L.M., 2019. Heterocyclic aromatic hydrocarbon distributions in petroleum: a source facies assessment tool. Org. Geochem. 137, 1–15. https://doi.org/10.1016/j.orggeochem.2019.07.005.

Azevedo, D.A., Neto, F.R.A., Simoneit, B.R.T., et al., 1992. Novel series of tricyclic aromatic terpanes characterized in Tasmanian tasmanite. Org. Geochem. 18, 9–16. https://doi.org/10.1016/0146-6380(92)90138-N.

Barnes, M.A., Barnes, W.C., 1983. Oxic and anoxic diagenesis of diterpenes in lacustrine sediments. Adv. Org. Geochem. 289–298.

Blumenberg, M., Arp, G., Reitner, J., et al., 2013. Bacteriohopanepolyols in a stratified cyanobacterial mat from Kiritimati (Christmas Island, Kiribati). Org. Geochem. 55, 55–62. https://doi.org/10.1016/j.orggeochem.2012.11.004.

Budzinsky, H., Garriges, P., Radke, M., et al., 1995. Alkylated phenanthrene distribution as maturity and source indicators in crude oils, rocks and artificially matured samples. Geochem. Cosmochim. Acta 59, 2043–2056. https://doi.org/10.1016/0016-7037(95)00125-5.

Connan, J., Bouroullec, J., Dessort, D., et al., 1986. The microbial input in carbonate-anhydrite facies of a sabkha palaeoenvironment from Guatemala A molecular approach. Org. Geochem. 10, 29–50. https://doi.org/10.1016/0146-6380(86)90007-0.

Damsté, J.S.S., Kenig, F., Koopmans, M.P., et al., 1995. Evidence for gammacerane as an indicator of water column stratification. Geochem. Cosmochim. Acta 59, 1895–1900. https://doi.org/10.1016/0016-7037(95)00073-9.

Ding, W.J., Hou, D.J., Gan, J., et al., 2021. Palaeovegetation variation in response to the late oligocene-early Miocene east asian summer monsoon in the ying-qiong basin, South China sea. Palaeogeogr. Palaeocl. 567, 1–24. https://doi.org/10.1016/j.palaeo.2020.110205.

Ding, W.J., Hou, D.J., Gan, J., et al., 2022. Aromatic hydrocarbon signatures of the late miocene-early pliocene in the Yinggehai Basin, South China sea: implications for climate variations. Mar. Petrol. Geol. 142, 1–23. https://doi.org/10.1016/j.marpetgeo.2022.105733.

Elling, F.J., Hemingway, J.D., Kharbush, J.J., et al., 2021. Linking diatom-diazotroph symbioses to nitrogen cycle perturbations and deep-water anoxia: insights from Mediterranean sapropel events. Earth Planet Sci. Lett. 571, 1–11. https://doi.org/10.1016/j.epsl.2021.117110.

Ellis, L., Singh, R.K., Alexander, R., et al., 1995. Geosynthesis of organic compounds: III. Formation of alkyltoluenes and alkylxylenes in sediments. Geochem. Cosmochim. Acta 59, 5133–5140. https://doi.org/10.1016/0016-7037(95)00352-5.

Fan, P., Philp, R.P., Li, Z.X., et al., 1991. Biomarker distributions in crude oils and source rocks from different sedimentary environments. Chem. Geol. 93, 61–78. https://doi.org/10.1016/0009-2541(91)90064-X.

Galimov, E.M., 2006. Isotope organic geochemistry. Org. Geochem. 37, 1200–1262. https://doi.org/10.1016/j.orggeochem.2006.04.009.

George, S.C., 1992. Effect of igneous intrusion on the organic geochemistry of a siltstone and an oil shale horizon in the Midland Valley of Scotland. Org. Geochem. 18, 705–723. https://doi.org/10.1016/0146-6380(92)90097-H.

Hayes, D.E., Nissen, S.S., 2005. The South China Sea margins: implications for rifting contrasts. Earth Planet Sci. Lett. 237, 601–616. https://doi.org/10.1016/j.epsl.2005.06.017.

Hayes, J.M., Takigiku, R., Ocampo, R., et al., 1987. Isotopic compositions and probable origins of organic molecules in the Eocene Messel shale. Nature 329, 48–51. https://doi.org/10.1038/329048a0.

Hill, R.J., Tang, Y.C., Kaplan, I.R., 2003. Insights into oil cracking based on laboratory experiments. Org. Geochem. 34, 1651–1672. https://doi.org/10.1016/s0146-6380(03)00173-6.

Huang, B.J., Hao, F., Wang, Z.F., et al., 2015. Kinetics and model of gas generation of source rocks in the deep-water area, Qiongdongnan Basin. Acta Oceanol. Sin. 34, 11–18. https://doi.org/10.1007/s13131-015-0646-3.

Huang, B.J., Tian, H., Li, X.S., et al., 2016. Geochemistry, origin and accumulation of

natural gases in the deepwater area of the Qiongdongnan Basin, South China Sea. Mar. Petrol. Geol. 72, 254–267. https://doi.org/10.1016/j.marpetgeo.2016.02.007.
Huang, B.J., Xiao, X.M., Li, X.X., 2003. Geochemistry and origins of natural gases in the Yinggehai and Qiongdongnan basins, offshore South China Sea. Org. Geochem. 34, 1009–1025. https://doi.org/10.1016/s0146-6380(03)00036-6.
Huang, H.T., Huang, B.J., Huang, Y.W., et al., 2017. Condensate origin and hydrocarbon accumulation mechanism of the deepwater giant gas field in western South China Sea: a case study of Lingshui 17-2 gas field in Qiongdongnan Basin. Petrol. Explor. Dev. 44, 409–417. https://doi.org/10.1016/S1876-3804(17)30047-2.
Huang, W.Y., Meinschein, W.G., 1979. Sterols as ecological indicators. Geochem. Cosmochim. Acta 43, 739–745. https://doi.org/10.1016/0016-7037(79)90257-6.
Hughes, W.B., Holba, A.G., Dzou, L.I.P., 1995. The ratios of dibenzothiophene to phenanthrene and pristane to phytane as indicators of depositional environment and lithology of petroleum source rocks. Geochem. Cosmochim. Acta 59, 3581–3598. https://doi.org/10.1016/0016-7037(95)00225-O.
Hutchison, C.S., 2004. Marginal basin evolution: the southern South China Sea. Mar. Petrol. Geol. 21, 1129–1148. https://doi.org/10.1016/j.marpetgeo.2004.07.002.
Jiang, C.Q., Alexander, R., Kagi, R.I., et al., 1998. Polycyclic aromatic hydrocarbons in ancient sediments and their relationships to palaeoclimate. Org. Geochem. 29, 1721–1735. https://doi.org/10.1016/s0146-6380(98)00083-7.
Karp, A.T., Holman, A.I., Hopper, P., et al., 2020. Fire distinguishers: refined interpretations of polycyclic aromatic hydrocarbons for paleo-applications. Geochem. Cosmochim. Acta 289, 93–113. https://doi.org/10.1016/j.gca.2020.08.024.
Kharbush, J.J., Thompson, L.R., Haroon, M.F., et al., 2018. Hopanoid-producing bacteria in the Red Sea include the major marine nitrite oxidizers. FEMS Microbiol. Ecol. 94, 1–9. https://doi.org/10.1093/femsec/fiy063.
Killops, S.D., Massoud, M.S., 1992. Polycyclic aromatic hydrocarbons of pyrolytic origin in ancient sediments evidence for Jurassic vegetation fires. Org. Geochem. 18, 1–7. https://doi.org/10.1016/0146-6380(92)90137-M.
Kodner, R.B., Pearson, A., Summons, R.E., et al., 2008. Sterols in red and green algae: quantification, phylogeny, and relevance for the interpretation of geologic steranes. Geobiology 6, 411–420. https://doi.org/10.1111/j.1472-4669.2008.00167.x.
Kump, L.R., Arthur, M.A., 1999. Interpreting carbon-isotope excursions carbonates and organic matter. Chem. Geol. 16, 181–198. https://doi.org/10.1016/S0009-2541(99)00086-8.
Kusch, S., Rush, D., 2022. Revisiting the precursors of the most abundant natural products on Earth: a look back at 30+ years of bacteriohopanepolyol (BHP) research and ahead to new frontiers. Org. Geochem. 172, 1–21. https://doi.org/10.1016/j.orggeochem.2022.104469.
Laflamme, R.E., Hites, R.A., 1978. The global distribution of polycyclic aromatic hydrocarbons in recent sediments. Geochem. Cosmochim. Acta 42, 289–303. https://doi.org/10.1016/0016-7037(78)90182-5.
Lamb, A.L., Wilson, G.P., Leng, M.J., 2006. A review of coastal palaeoclimate and relative sea-level reconstructions using δ13C and C/N ratios in organic material. Earth Sci. Rev. 75, 29–57. https://doi.org/10.1016/j.earscirev.2005.10.003.
Lai, H.F., Fang, Y.X., Kuang, Z.G., et al., 2021. Geochemistry, origin and accumulation of natural gas hydrates in the Qiongdongnan Basin, South China Sea: implications from site GMGS5-W08. Mar. Petrol. Geol. 123, 1–14. https://doi.org/10.1016/j.marpetgeo.2020.104774.
Lei, C., Ren, J.Y., Li, X.S., et al., 2011. Structural characteristics and petroleum exploration potential in the deep-water area of the Qiongdongnan Basin, South China Sea. Petrol. Explor. Dev. 38, 560–568. https://doi.org/10.3799/dqkx.2011.016.
Li, M.J., Wang, T.G., Zhong, N.N., et al., 2013. Ternary diagram of fluorenes, dibenzothiophenes and dibenzofurans: indicating depositional environment of crude oil source rocks. Energy Explor. Exploit. 31, 569–588. https://doi.org/10.1260/0144-5987.31.4.569.
Li, W.H., Zhang, Z.H., 2017. Paleoenvironment and its control of the formation of Oligocene marine source rocks in the deep-water area of the Northern South China Sea. Energy Fuels 31, 10598–10611. https://doi.org/10.1021/acs.energyfuels.7b01681.
Liang, G., Gan, J., Li, X., 2015. Genetic types and origin of natural gas in Lingshui sag, Qiongdongnan Basin. China Offshore Oil Gas 27, 47–53.
Lis, G.P., Mastalerz, M., Schimmelmann, A., 2008. Increasing maturity of kerogen type II reflected by alkylbenzene distribution from pyrolysis-gas chromatography–mass spectrometry. Org. Geochem. 39, 440–449. https://doi.org/10.1016/j.orggeochem.2008.01.007.
Liu, K., Cheng, P., Fan, C.W., et al., 2023. Evolutions of sedimentary facies and palaeoenvironment and their controls on the development of source rocks in continental margin basins: a case study from the Qiongdongnan Basin, South China Sea. Petrol. Sci. 20, 2648–2663. https://doi.org/10.1016/j.petsci.2023.04.019.
Liu, X.B., Liu, G.D., Jiang, W.Y., et al., 2022. Org. Geochem and petrology of source rocks from the banqiao sag, bohai bay basin, China: implications for petroleum exploration. Petrol. Sci. 19, 1505–1515. https://doi.org/10.1016/j.petsci.2022.07.002.
Mackensen, A., Schmiedl, G., 2019. Stable carbon isotopes in paleoceanography: atmosphere, oceans, and sediments. Earth Sci. Rev. 197, 1–23. https://doi.org/10.1016/j.earscirev.2019.102893.
Moldowan, J.M., Dahl, J., Huizinga, B.J., et al., 1994. The molecular fossil record of oleanane and its relation to angiosperms. Science 265, 768–771. https://doi.org/10.1126/science.265.5173.768.
Moldowan, J.M., Seifert, W.K., Gallegos, E.J., 1985. Relationship between petroleum composition and depositional environment of petroleum source rocks. AAPG Bull. 69, 1255–1268. https://doi.org/10.1306/AD462BC8-16F7-11D7-8645000102C1865D.
Murray, A.P., Sosrowidjojo, I.B., Alexander, R., et al., 1997. Oleananes in oils and sediments: evidence of marine influence during early diagenesis? Geochem. Cosmochim. Acta 61, 1261–1276. https://doi.org/10.1016/S0016-7037(96)00408-5.
Murray, A.P., Edwards, D., Hope, J.M., et al., 1998. Carbon isotope biogeochemistry of plant resins and derived hydrocarbons. Org. Geochem. 29, 1199–1214. https://doi.org/10.1016/S0146-6380(98)00126-0.
Nytoft, H.P., Kildahl-Andersen, G., Samuel, O.J., 2010. Rearranged oleananes: structural identification and distribution in a worldwide set of Late Cretaceous/Tertiary oils. Org. Geochem. 41, 1104–1118. https://doi.org/10.1016/j.orggeochem.2010.06.008.
Peters, K.E., Moldowan, J.M., 1991. Effect of source, thermal maturity, and biodegradation on the distribution and isomerization of homohopanes in petroleum. Org. Geochem. 17, 47–61. https://doi.org/10.1016/0146-6380(91)90039-M.
Peters, K.E., Walters, C.C., Moldowan, J.M., 2005. The Biomarker Guide: Biomarkers and Isotopes in Petroleum Exploration and Earth History, 2 ed. Cambridge University Press, Cambridge. https://doi.org/10.1017/CBO9781107326040.
Philp, R.P., Gilbert, T.D., 1982. Unusual distribution of biological markers in an Australian crude oil. Nature 299, 245–247. https://doi.org/10.1038/299245a0.
Püttmann, W., Villar, H., 1987. Occurrence and geochemical significance of 1,2,5,6-tetra-methylnaphthalene. Geochem. Cosmochim. Acta 51, 3023–3029. https://doi.org/10.1016/0016-7037(87)90375-9.
Radke, M., Vriend, S.P., Ramanampisoa, L.R., 2000. Alkyldibenzofurans in terrestrial rocks influence of organic facies and maturation. Geochem. Cosmochim. Acta 64, 275–286. https://doi.org/10.1016/S0016-7037(99)00287-2.
Radke, M., Welte, D.H., Willsch, H., 1982. Geochemical study on a well in the Western Canada Basin relation of the aromatic distribution pattern to maturity of organic matter. Geochem. Cosmochim. Acta 46, 1–10. https://doi.org/10.1016/0016-7037(82)90285-X.
Radke, M., Willsch, H., 1993. Generation of alkylbenzenes and benzo[b]thiophenes by artificial thermal maturation of sulfur-rich coal. Fuel 72, 1103–1108. https://doi.org/10.1016/0016-2361(93)90316-T.
Richey, J.D., Nordt, L., White, J.D., et al., 2023. ISOORG23: an updated compilation of stable carbon isotope data of terrestrial organic materials for the Cenozoic and Mesozoic. Earth Sci. Rev. 241. https://doi.org/10.1016/j.earscirev.2023.104439.
Riolo, J., Hussler, G., Albrecht, P., et al., 1986. Distribution of aromatic steroids in geological samples: their evaluation as geochemical parameters. Org. Geochem. 10, 981–990. https://doi.org/10.1016/S0146-6380(86)80036-5.
Samuel, O.J., Kildahl-Andersen, G., Nytoft, H.P., et al., 2010. Novel tricyclic and tetracyclic terpanes in Tertiary deltaic oils: structural identification, origin and application to petroleum correlation. Org. Geochem. 41, 1326–1337. https://doi.org/10.1016/j.orggeochem.2010.10.002.
Schidlowski, M., Matzigkeit, U., Krumbein, W., 1984. Superheavy organic carbon from hypersaline microbial mats. Naturwissenschaften 71, 303–308. https://doi.org/10.1007/BF00396613.
Schoell, M., Hwang, R.J., Carlson, R.M.K., et al., 1994. Carbon isotopic composition of individual biomarkers in gilsonites (Utah). Org. Geochem. 21, 673–683. https://doi.org/10.1016/0146-6380(94)90012-4.
Simoneit, B.R.T., Grimalt, J.O., Wang, T.G., et al., 1986. Cyclic terpenoids of contemporary resinous plant detritus and of fossil woods, ambers and coals. Org. Geochem. 10, 877–889. https://doi.org/10.1016/S0146-6380(86)80025-0.
Sofer, Z., 1984. Stable carbon isotope compositions of crude oils: application to source depositional environments and petroleum alteration. AAPG Bull. 68, 31–49. https://doi.org/10.1306/AD460963-16F7-11D7-8645000102C1865D.
Strachan, M.G., Alexander, R., Kagi, R.I., 1988. Trimethylnaphthalenes in crude oils and sediments: effects of source and maturity. Geochem. Cosmochim. Acta 52, 1255–1264. https://doi.org/10.1016/0016-7037(88)90279-7.
Summons, R.E., Brassell, S.C., Eglinton, G., et al., 1988. Distinctive hydrocarbon biomarkers from fossiliferous sediment of the late proterozoic walcott member, chuar group, grand canyon, Arizona. Geochem. Cosmochim. Acta 52, 2625–2637. https://doi.org/10.1016/0016-7037(88)90031-2.
Summons, R.E., Jahnke, L.L., Hope, J.M., et al., 1999. 2-Methylhopanoids as biomarkers for cyanobacterial oxygenic photosynthesis. Nature 400, 554–557. https://doi.org/10.1038/23005.
Tian, C.T., Chen, Y.X., Xia, Y.Q., et al., 2018. Characterisation of aromatic hydrocarbons formed from alkane pyrolysis. Geochem. J. 52, 335–345. https://doi.org/10.2343/geochemj.2.0521.
van Aarssen, B.G.K., Alexander, R., Kagi, R.I., 2000. Higher plant biomarkers reflect palaeovegetation changes during Jurassic times. Geochem. Cosmochim. Acta 64, 1417–1424. https://doi.org/10.1016/S0016-7037(99)00432-9.
van Aarssen, B.G.K., Cox, H.C., Hoogendoorn, P., et al., 1990. A cadinene biopolymer in fossil and extant dammar resins as a source for cadinanes and bicadinanes in crude oils from South East Asia. Geochem. Cosmochim. Acta 54, 3031. https://doi.org/10.1016/0016-7037(90)90119-6, 3031.
Versteegh, G.J.M., Schefuß, E., Dupont, L., et al., 2004. Taraxerol and Rhizophora pollen as proxies for tracking past mangrove ecosystems. Geochem. Cosmochim. Acta 68, 411–422. https://doi.org/10.1016/S0016-7037(03)00456-3.
Volkman, J.K., 1986. A review of sterol markers for marine and terrigenous organic matter. Org. Geochem. 9, 83–99. https://doi.org/10.1016/0146-6380(86)90089-6.
Wang, D.D., Dong, G.Q., Zhang, G.C., et al., 2020. Coal seam development

characteristics and distribution predictions in marginal sea basins: Oligocene Yacheng Formation coal measures, Qiongdongnan Basin, northern region of the South China Sea. Aust. J. Earth Sci. 67, 393–409. https://doi.org/10.1080/08120099.2019.1661286.

Wang, G.L., Wang, T.G., Zhang, L.Y., et al., 2006. 2-Methylhopanes as biomarkers for depositional environment in the lacustrine basin. Acta Geol. Sin. 80, 902–909. https://doi.org/10.3321/j.issn:0001-5717.2006.06.012.

Wang, Z.F., Liu, Z., Cao, S., et al., 2014. Vertical migration through faults and hydrocarbon accumulation patterns in deepwater areas of the Qiongdongnan Basin. Acta Oceanol. Sin. 33, 96–106. https://doi.org/10.1007/s13131-014-0579-2.

Wójcik-Tabol, P., Wendorff-Belon, M., Kosakowski, P., et al., 2022. Paleoenvironment, organic matter maturity and the hydrocarbon potential of Menilite shales (Silesian Unit, Polish Outer Carpathians)—Organic and inorganic geochemical proxies. Mar. Petrol. Geol. 142, 1–22. https://doi.org/10.1016/j.marpetgeo.2022.105767.

Wu, P., Hou, D.J., Gan, J., et al., 2018. Paleoenvironment and controlling factors of Oligocene source rock in the Eastern deep-water area of the Qiongdongnan basin: evidences from organic geochemistry and palynology. Energy Fuels 32, 7423–7437. https://doi.org/10.1021/acs.energyfuels.8b01190.

Xiao, X.M., Xiong, M., Tian, H., et al., 2006. Determination of the source area of the ya13-1 gas pool in the Qiongdongnan Basin, South China sea. Org. Geochem. 37, 990–1002. https://doi.org/10.1016/j.orggeochem.2006.06.001.

Xiong, X., Guo, X., Zhu, J., et al., 2019. Causes of natural gas geochemical differences in the deep water area gas field, western South China Sea. Nat. Gas Geosci. 30, 1053–1062. https://doi.org/10.11764/j.issn.1672-1926.2019.04.010.

Xu, C.G., Deng, Y., Wu, K.Q., et al., 2023a. Discovery and geological significance of the large gas field Baodao 21-1 in a passive epicontinental basin with strong activity in the northern South China Sea. Acta Petrolei 44, 713–728. https://doi.org/10.7623/syxb202305001. Sin.

Xu, M., Hou, D., Cheng, X., et al., 2023b. Aliphatic biomarker signatures of early Oligocene—early Miocene source rocks in the central Qiongdongnan Basin: source analyses of organic matter. Acta Oceanol. Sin. 42, 1–18. https://doi.org/10.1007/s13131-022-2082-5.

Yunker, M.B., Macdonald, R.W., Vingarzan, R., et al., 2002. PAHs in the Fraser River basin: a critical appraisal of PAH ratios as indicators of PAH source and composition. Org. Geochem. 33, 489–515. https://doi.org/10.1016/S0146-6380(02)00002-5.

Zhou, D., Sun, Z., Chen, Z.H., et al., 2008. Mesozoic paleogeography and tectonic evolution of South China Sea and adjacent areas in the context of Tethyan and Paleo-Pacific interconnections. Isl. Arc 17, 186–207. https://doi.org/10.1111/j.1440-1738.2008.00611.x.

Zhou, Y., Sheng, G.Y., Fu, J.M., et al., 2003. Triterpane and sterane biomarkers in the YA13-1 condensates from Qiongdongnan Basin, South China sea. Chem. Geol. 199, 343–359. https://doi.org/10.1016/s0009-2541(03)00123-2.

Zhu, W.L., Huang, B.J., Mi, L.J., et al., 2009. Geochemistry, origin, and deep-water exploration potential of natural gases in the Pearl River Mouth and Qiongdongnan basins, South China Sea. AAPG Bull. 93, 741–761. https://doi.org/10.1306/02170908099.

Zhu, W.L., Shi, H.S., Huang, B.J., et al., 2021. Geology and geochemistry of large gas fields in the deepwater areas, continental margin basins of northern South China Sea. Mar. Petrol. Geol. 126, 1–15. https://doi.org/10.1016/j.marpetgeo.2021.104901.

Zhu, Y.M., Sun, L.T., Hao, F., et al., 2018. Geochemical composition and origin of tertiary oils in the Yinggehai and qiongdongnan basins, offshore South China sea. Mar. Petrol. Geol. 96, 139–153. https://doi.org/10.1016/j.marpetgeo.2018.05.029.